AIR ATOMIZATION OF FUEL OIL

SUBMITTED BY:
LT. P.F. ERKENBRACK, U.S.NAVY
LT. R.J. ZOELLER, U.S.NAVY

THESIS SUPERVISOR:
PROFESSOR H.C. HOTTEL

JANUARY 16,1948

AIR ATOMIZATION OF FUEL OIL

by

Lieutenant Phillip Frederick ErkenBrack, U. S. Navy
B.S., U. S. Naval Academy, 1942

Lieutenant Robert Joseph Zoeller, U. S. Navy
B.S., U. S. Naval Academy, 1942

Submitted in Partial Fulfillment of the

Requirements for the Degree of

MASTER OF SCIENCE

in

NAVAL CONSTRUCTION AND ENGINEERING

from the

MASSACHUSETTS INSTITUTE OF TECHNOLOGY

1948

Cambridge,
Massachusetts,
January 16, 1948.

Professor J. S. Newell,
Secretary of the Faculty,
Massachusetts Institute of Technology,
Cambridge, Massachusetts.

Dear Sir:

In accordance with the requirements for the Degree of Master of Science in Naval Construction and Engineering, we submit herewith a thesis entitled "AIR ATOMIZATION OF FUEL OIL".

Respectfully,

ACKNOWLEDGMENT

The authors wish to express their appreciation for the assistance and advice of Professor Hoyt C. Hottel who suggested the subject, and under whose supervision the investigation was conducted.

ACKNOWLEDGMENT

The authors wish to express their appreciation for the assistance and advice of Professor Hoyt C. Hottel who suggested the subject, and under whose supervision the investigation was conducted.

TABLE OF CONTENTS

SUMMARY

This thesis presents a macroscopic study of the effect of orifice diameter, fuel rate, air velocity and type of injection on the characteristics of a spray of fuel oil atomized by a high velocity air stream. The qualitative results were obtained from a close examination of photographs taken both by normal exposure technique and by use of the Edgerton high speed spark-lighting technique. The sprays investigated were those of U. S. Navy Diesel oil injected into an air stream in three ways: (a) Parallel to and in the direction of air stream flow; (b) perpendicular to the direction of air stream flow; and (c) parallel to and counter to the direction of air stream flow.

The results show that normal photographic procedure with time exposure to portray a spray envelope is of little value in studying atomization characteristics and, in fact, leaves erroneous impressions. Spark photography, on the other hand, gives excellent qualitative information and has possibilities for some quantitative development.

It was found that:

(a) For increasing orifice diameter, drop size and uniformity were not materially affected, dispersion increased.

(b) For increasing air velocity, drop size and dispersion decreased and uniformity increased.

(c) For increased fuel rate, uniformity and dispersion decreased and drop size increased at low air velocities and was not affected materially at high velocities.

(d) For type of injection, spray characteristics were not materially affected.

Perpendicular and upstream injection offer serious disadvantages in the way of fuel nozzle distortion of the air stream. From all considerations, downstream injection from large orifices affords the best atomization. This is fortunate for in application to modern high rate combustion chambers, it means maximum flexibility with moderate pump size.

INTRODUCTION

With recent increased interest in, and development of, high rate combustion chambers, studies of the atomization of liquid fuels by a high velocity air stream have assumed new importance. Jet, and turbo-jet engines, and gas turbines have available a high velocity air stream as an inherent part of the design which is most efficiently used as a fuel atomizing force. At present, insufficient knowledge of the variables and controlling factors of air atomization prevents a wholly scientific attack on the design problem with the consequent result that much of the combustion planning is done on a trial and error, or rule of thumb, basis.

Fuels are atomized mechanically by "solid injection", or by a gas stream. In the former, the liquid is atomized by forcing it under high pressure through a small orifice of special design into a stagnant gas. In the latter, the liquid is atomized by the shearing action of a high velocity gas stream on the surface of the liquid column as it is pumped from an orifice under just sufficient pressure to give the desired fuel rate.

Until quite recently, air atomization has always given way to pressure atomization in the combustion of fuel oils because of the high efficiency of pressure systems, the relatively simple problem of putting fuel under pressure and preheating it, and the unnecessarily complicated design

problem of compressing large quantities of air and controlling the velocities required for proper atomization. However, the demand of modern power systems for compactness, lightness, simplicity, dependability, and most important, extreme flexibility, has shifted attention to atomization by an air stream. As the range of fuel rates increases in a pressure atomization system, the pressure required (and, consequently, the size and weight of pump) increases in far greater proportion - the fuel rate being proportional to the square of the fuel oil pressure.

Because of the tremendous scope of the field and the pressing need for specific information, a great deal of the research work on the subject of atomization pertains to commercial arrangements tested under fixed conditions. Also, because the characteristics of a liquid spray are so difficult to measure experimentally with accuracy, most of the work is of a qualitative nature. The meager quantitative data available to date is empirical in nature and investigators are generally in poor agreement. Some theoretical considerations have been made, but these, too, are meager.

In the literature, information is extremely sparse on the effect of orifice diameter on the spray characteristics of an atomized liquid. Longwell (11) has shown that drop size increases with increasing orifice diameter and decreases with fuel velocity at the orifice, the velocity being a function of the pressure, but this applies only to solid injection using swirl-type nozzles. It is reasoned that penetration problem of compressing large quantities of air and controlling the velocities required for proper atomization. However, the demand of modern power systems for compactness, lightness, simplicity, dependability, and most important, extreme flexibility, has shifted attention to atomization by an air stream. As the range of fuel rates increases in a pressure atomization system, the pressure required (and, consequently, the size and weight of pump) increases in far greater proportion - the fuel rate being proportional to the square of the fuel oil pressure.

Because of the tremendous scope of the field and the pressing need for specific information, a great deal of the research work on the subject of atomization pertains to commercial arrangements tested under fixed conditions. Also, because the characteristics of a liquid spray are so difficult to measure experimentally with accuracy, most of the work is of a qualitative nature. The meager quantitative data available to date is empirical in nature and investigators are generally in poor agreement. Some theoretical considerations have been made, but these, too, are meager.

In the literature, information is extremely sparse on the effect of orifice diameter on the spray characteristics of an atomized liquid. Longwell (11) has shown that drop size increases with increasing orifice diameter and decreases with fuel velocity at the orifice, the velocity being a function of the pressure, but this applies only to solid injection using swirl-type nozzles. It is reasoned that penetration increases with decreasing orifice diameter, but even qualitative substantiation is lacking. It is known that orifice geometry is the most controlling factor for dispersion and spray intensity, but there is no information as to how orifice size affects them. It is felt, then, that an investigation of even a qualitative nature could add much to the knowledge of atomization in general, and to air atomization of liquid fuels in particular.

With this in mind, this thesis is concerned with studying the effect of orifice diameter on the characteristics of a spray of diesel oil formed by air atomization under varying and controlled conditions of air and fuel rate. For this purpose, a series of nozzles were photographed by the Edgerton Spark technique and, where feasible, by time exposure on the spray envelope at each of six conditions of fuel and air rate, and the results macroscopically compared.

increases with decreasing orifice diameter, but even qualitative substantiation is lacking. It is known that orifice geometry is the most controlling factor for dispersion and spray intensity, but there is no information as to how orifice size effects them. It is felt, then, that an investigation of even a qualitative nature could add much to the knowledge of atomization in general, and to air atomization of liquid fuels in particular.

With this in mind, this thesis is concerned with studying the effect of orifice diameter on the characteristics of a spray of diesel oil formed by air atomization under varying and controlled conditions of air and fuel rate. For this purpose, a series of nozzles were photographed by the Edgerton Spark technique and, where feasible, by time exposure on the spray envelope at each of six conditions of fuel and air rate, and the results macroscopically compared.

PROCEDURE

Description of Apparatus

The apparatus used was originally designed and constructed by Geoffrey Robillard (14), later modified by Robert Maxwell of the M.I.T. Combustion Research Laboratory, and finally modified for this thesis by the authors. It is designed to take high speed photographs of a liquid spray. A schematic arrangement of the apparatus is shown in Figure I. Figure II shows all the actual apparatus, with the exception of the air compressor, while Figure III is a close-up of the chamber.

The focus of the investigation is on a diesel oil spray contained in a glass chamber, and for obtaining and photographing this spray, three systems are necessary: the air system, the fuel system, and the photographic system.

The Air System: Air from a 100 psi, 533 cfm Allis Chalmers "RoTwin" gear type compressor flows through a two-inch pipe past a one-inch orifice for measuring air rate. The air then flows through a diffuser in which is a four-inch square section containing three fifty mesh screens in series which minimize turbulence and maximize a uniform velocity front. The diffuser exit is reduced through a nozzle to a one square inch cross section. The nozzle outlet is directly connected to the spray chamber. This chamber consists of two one-quarter inch thick optical flats and two one-quarter inch thick milled steel plates. These plates and flats form a

PROCEDURE

Description of Apparatus

The apparatus used was originally designed and constructed by Geoffrey Robillard (14), later modified by Robert Maxwell of the M.I.T. Combustion Research Laboratory, and finally modified for this thesis by the authors. It is designed to take high speed photographs of a liquid spray. A schematic arrangement of the apparatus is shown in Figure I. Figure II shows all the actual apparatus, with the exception of the air compressor, while Figure III is a close-up of the chamber.

The focus of the investigation is on a diesel oil spray contained in a glass chamber, and for obtaining and photographing this spray, three systems are necessary: the air system, the fuel system, and the photographic system.

The Air System: Air from a 100 psi, 533 cfm Allis Chalmers "RoTwin" gear type compressor flows through a two-inch pipe past a one-inch orifice for measuring air rate. The air then flows through a diffuser in which is a four-inch square section containing three fifty mesh screens in series which minimize turbulence and maintain a uniform velocity front. The diffuser exit is reduced through a nozzle to a one square inch cross section. The nozzle outlet is directly connected to the spray chamber. This chamber consists of two one-quarter inch thick optical flats and two one-quarter inch thick milled steel plates. These plates and flats form a square duct one inch on a side, inside dimension, and six inches in length, two opposing walls of which are perfectly transparent. The outlet of the spray chamber is connected to a two-inch exhaust line.

The spray chamber walls, when secured by thumb screws into aluminum blocks at each end, form a rigidly intact unit which slides into brass guide blocks secured to the nozzle exit and exhaust duct. The chamber is then secured in place by raising the lower guide block by means of a threaded collar.

Air temperature is measured at a thermometer well preceding the diffuser. Static pressure in the section between diffuser and nozzle is measured by manometer and calibrated against chamber pressure, as described in Appendix E. Static pressure downstream of the metering orifice and differential pressure across the orifice are measured by manometer.

A by-pass line from a point preceding the metering orifice to the exhaust duct contains a stop valve by means of which air rate is controlled. Air velocities from 125 to 830 feet per second can be attained in the chamber.

<u>The Fuel System</u>: Fuel is supplied from a five gallon reservoir by a "Gerator" gear pump capable of 150 psi and equipped with internal by-passes. The fuel is metered through a 0.025-inch orifice in half-inch brass tubing and measured by a fuel-over-mercury manometer independently calibrated, as described in Appendix E.

The fuel is introduced into the chamber through a brass adapter which holds the nozzle under investigation. One end of the adapter accommodates the fuel line; the other end screws into a tapped hole in one of the metal walls of the chamber, as indicated in Figure IV. The adapter is held securely in place by means of two lock washers and a nut.

The two sets of five nozzles, ranging in inside diameter from 0.023 to 0.105 inches, are Stainless steel tubing of the type used for hypodermic needles. The word nozzle is used only for convenience, and carries no implications of having converging or diverging sections, as no attempt was made to alter the character of flow at the discharge end of the fuel line other than that dictated by the differences in inside diameter. Each nozzle was silver soldered into the adapter, bent, ground and polished, as described in Appendix D.

Fuel rate is controlled by a globe valve preceding the metering orifice.

<u>The Photographic System</u>: Photographs are taken with a Voightlander 9 x 12 cm. film, f 4.5 pack camera equipped with a 7.5 cm. focal length lens and double extension bellows. The lighting and camera arrangement is shown in Figure III. Light is provided by discharging across a one-half inch stainless steel spark gap a 0.01 microfarad condenser charged to 15,000 volts by a simple half-wave rectifier using 60 cycle

The fuel is introduced into the chamber through a brass adapter which holds the nozzle under investigation. One end of the adapter accommodates the fuel line; the other end screws into a tapped hole in one of the metal walls of the chamber, as indicated in Figure IV. The adapter is held securely in place by means of two lock washers and a nut.

The two sets of five nozzles, ranging in inside diameter from 0.023 to 0.105 inches, are stainless steel tubing of the type used for hypodermic needles. The word nozzle is used only for convenience, and carries no implications of having converging or diverging sections, as no attempt was made to alter the character of flow at the discharge end of the fuel line other than that dictated by the differences in inside diameter. Each nozzle was silver soldered into the adapter, bent, ground and polished, as described in Appendix C.

Fuel rate is controlled by a globe valve preceding the metering orifice.

The Photographic System: Photographs are taken with a Voigtlander 9 x 12 cm. film, f 4.5 pack camera equipped with a 7.5 cm. focal length lens and double extension bellows. The lighting and camera arrangement is shown in Figure III. Light is provided by discharging across a one-half inch stainless steel spark gap a 0.01 microfarad condenser charged to 15,000 volts by a single half-wave rectifier using 60 cycle

SCHEMATIC DIAGRAM OF APPARATUS

FIGURE I

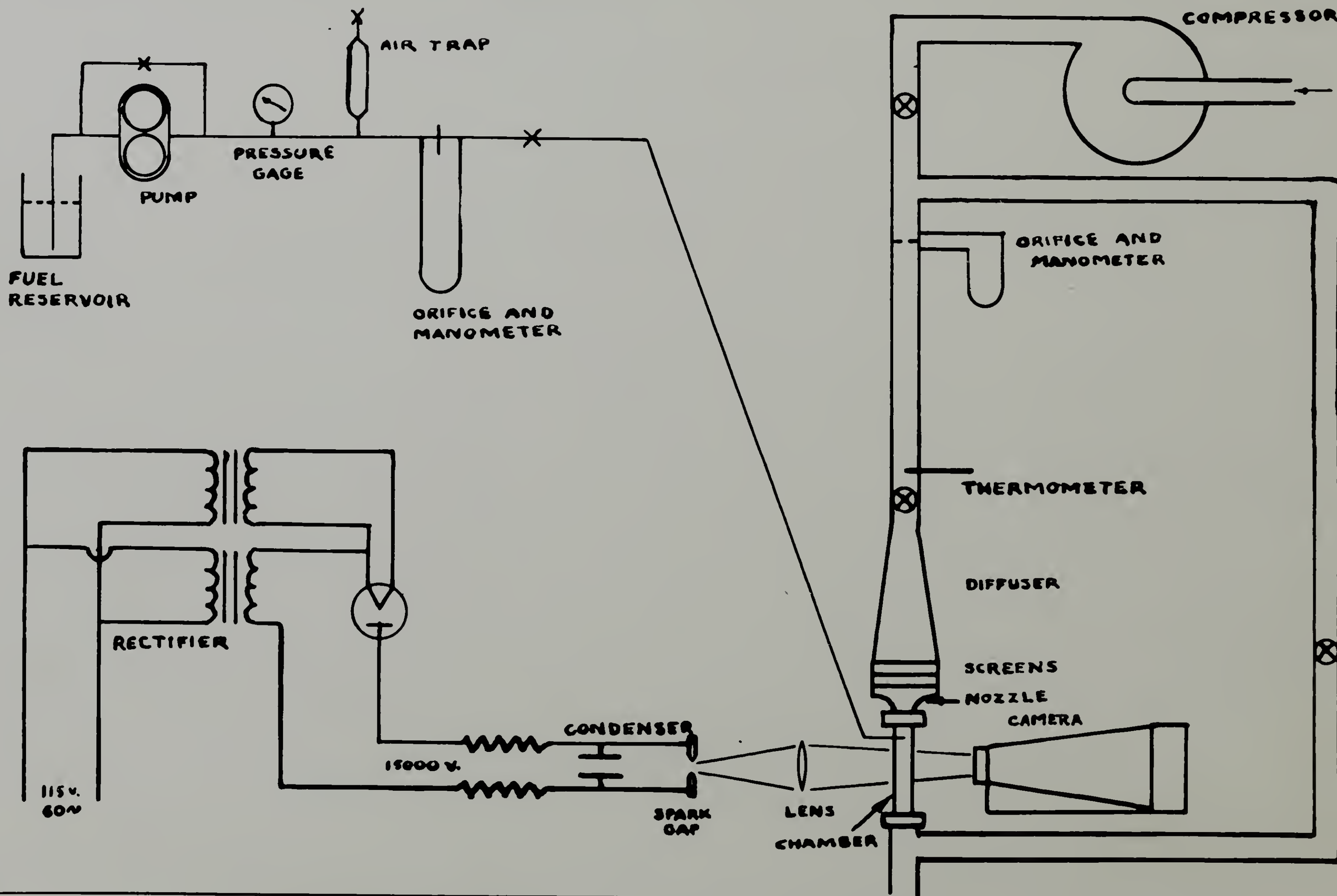

LEGEND FOR FIGURES II AND III

A. Air orifice meter.
B. Power pack.
C. Thermometer well.
D. Air by-pass valve.
E. Fuel control valve.
F. Fuel orifice meter.
G. Air trap.
H. Fuel pump by-pass valve and pressure gage.
I. Fuel pump.
J. Fuel Reservoir.
K. Diffuser.
L. Air rate manometer.
M. Fuel rate manometer.
N. Diffuser and Orifice Static pressure manometer.
O. Optical Bench and adjusting jacks.
P. Exit Duct.
Q. Variac.
R. Air Control valve.
S. Chamber.
T. Spark Gap.
U. Condenser.
V. Condensing lenses.
W. Mirror.
X. Fuel adapter and nozzle.
Y. Light-proof cloth.
Z. Camera.

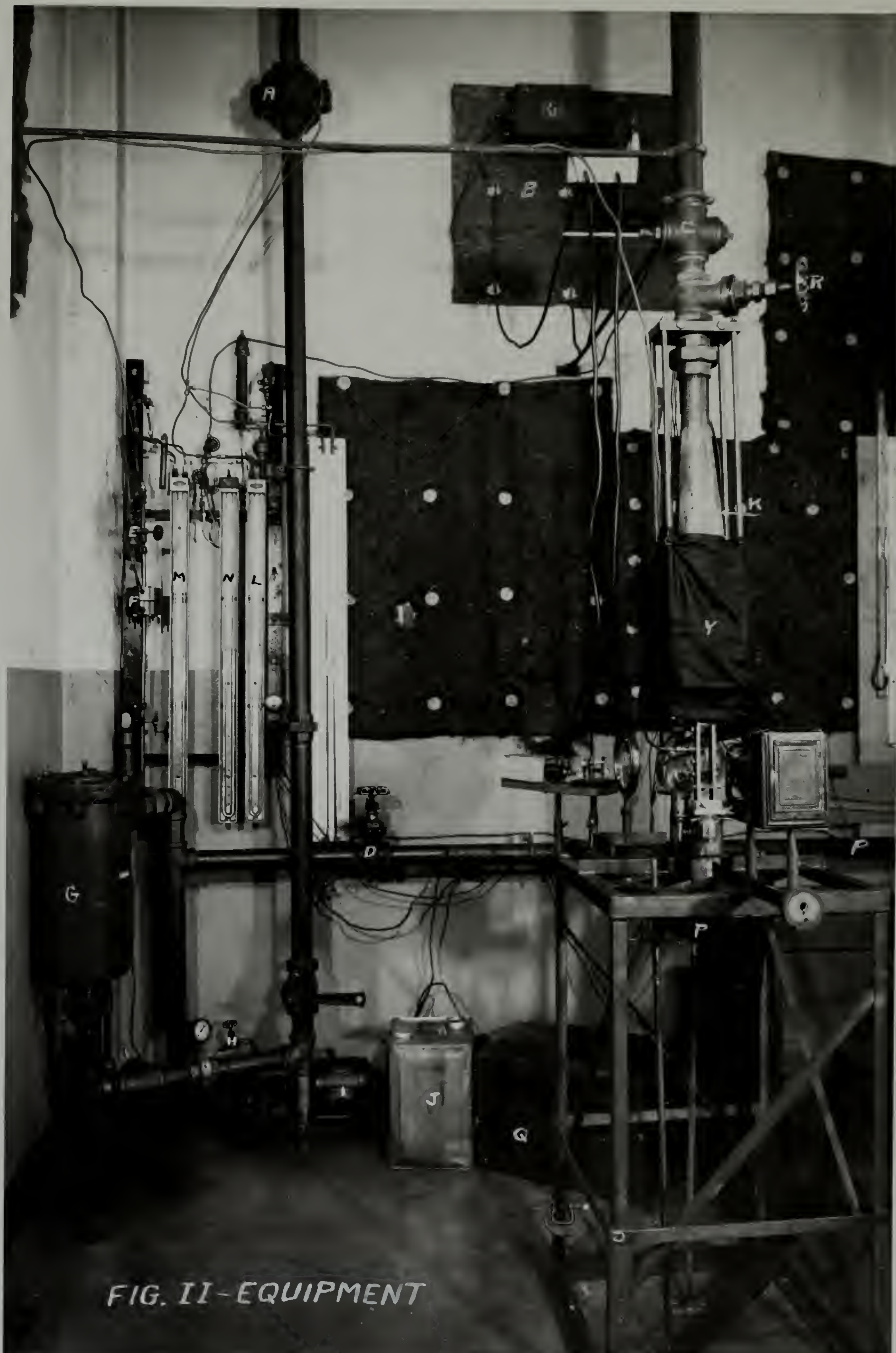

FIG. II - EQUIPMENT

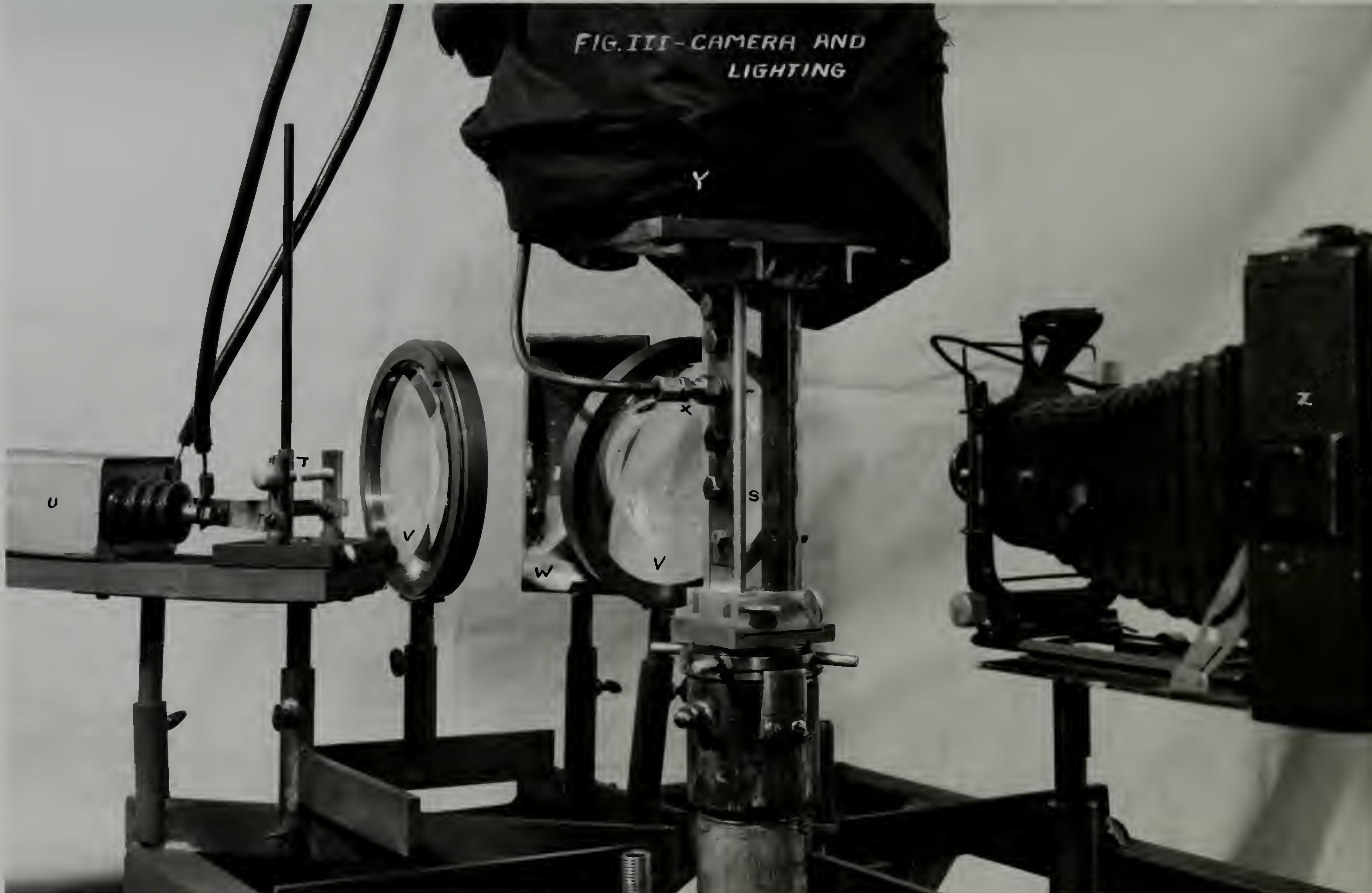
FIG. III - CAMERA AND LIGHTING
Y
T
U
V
W
V
X
S
Z

FIG. IV - FUEL NOZZLES

115 volt building power. This spark technique and the power pack design is fully described in (14). Previous measurements have shown the spark duration to be less than 0.25×10^{-7} seconds.

The light from the spark is directed by two five-inch condensing lenses and a 3 x 6 inch mirror into the camera through the chamber so that the spray is photographed in semi-silhouette. The light is diffused and centered by manipulation of the lenses.

The camera, spark gap, mirror and lenses are supported on a 24 x 24 inch bench with telescoping legs, which can be adjusted vertically by means of two screw-type jacks so that any part of the chamber may be photographed. The base is bolted rigidly to the floor.

A light-proof cloth cloaks the chamber, nearest condensing lens, and the camera lens so that the camera shutter may be opened, the condenser discharged,and the shutter closed, eliminating the necessity for spark-shutter synchronization.

Experimental Procedure

The oil spray was obtained with three types of fuel injection: downstream flow, perpendicular flow and upstream flow.

For downstream flow, the bent nozzle to be studied was secured in a tapped hole near the top of one metal wall, the chamber assembled and installed. The alignment of the nozzle in the plane of the adapter was checked when the nozzle

115 volt building power. This spark technique and the power pack design is fully described in [14]. Previous measurements have shown the spark duration to be less than 0.25×10^{-7} seconds.

The light from the spark is directed by two five-inch condensing lenses and a 3 x 6 inch mirror into the camera through the chamber so that the spray is photographed in semi-silhouette. The light is diffused and scattered by manipulation of the lenses.

The camera, spark gap, mirror and lenses are supported on a 24 x 24 inch bench with telescoping legs, which can be adjusted vertically by means of two screw-type jacks so that any part of the chamber may be photographed. The base is bolted rigidly to the floor.

A light-proof cloth cloaks the chamber, nearest condensing lens, and the camera lens so that the camera shutter may be opened, the condenser discharged, and the shutter closed, eliminating the necessity for spark-shutter synchronization.

Experimental Procedure

The oil spray was obtained with three types of fuel injection: downstream flow, perpendicular flow and upstream flow.

For downstream flow, the bent nozzle to be studied was secured in a tapped hole near the top of one metal wall, the chamber assembled and installed. The alignment of the nozzle in the plane of the adapter was checked when the nozzle and adapter were made (see Appendix D). The alignment in the line of sight of the camera was checked by opening a plugged hole in the opposite metal wall that was closest to the nozzle tip.

For perpendicular flow, disassembly of the chamber was not necessary and the nozzles could be inserted by merely screwing them into a tapped hole near the top until the forward face of the adapter was flush with the milled inner surface of the wall.

For upstream flow, the procedure was the same as for downstream flow except that the metal wall was reversed, top-to-bottom, with the nozzle pointing up into the chamber.

For each type of flow, and for each nozzle run at a specified condition of air and fuel rate, the procedure was as follows:

1. Camera and lenses were aligned and the bench was adjusted to proper height.
2. The air compressor was started and allowed to build up pressure until stable conditions existed in the surge tank with the by-pass open.
3. The fuel pump was started and pressure adjusted by internal by-pass to 90 psi.
4. The desired air rate was set by adjusting the by-pass.
5. The desired fuel rate was set by adjusting the fuel valve.
6. The light-proof cloth was adjusted around the chamber.

and adapter were made (see Appendix D). The alignment in the line of sight of the camera was checked by opening a plugged hole in the opposite metal wall that was closer to the nozzle tip.

For perpendicular flow, disassembly of the chamber was not necessary and the nozzles could be inserted by merely screwing them into a tapped hole near the top until the forward face of the adapter was flush with the milled inner surface of the wall.

For upstream flow, the procedure was the same as for downstream flow except that the metal wall was reversed, top-to-bottom, with the nozzle pointing up into the chamber.

For each type of flow, and for each nozzle run at a specified condition of air and fuel rate, the procedure was as follows:

1. Camera and lenses were aligned and the bench was adjusted to proper height.
2. The air compressor was started and allowed to build up pressure until stable conditions existed in the surge tank with the by-pass open.
3. The fuel pump was started and pressure adjusted by internal by-pass to 90 psi.
4. The desired air rate was set by adjusting the by-pass.
5. The desired fuel rate was set by adjusting the fuel valve.
6. The light-proof cloth was adjusted around the chamber.

7. The shutter was opened, condenser discharged, and shutter closed.

8. All manometers were read.

Each nozzle was photographed at a high and a low fuel rate and at a low, intermediate, and high air rate for each fuel rate.

For downstream flow, the spray envelope was photographed at each condition with reflected light from two Super Flood lamps placed 18 inches behind the camera lens and at the maximum angle permitted by the chamber walls. The exposure time was 2-4 seconds at f3.5.

RESULTS

The results are presented as a series of plates, Figures V through XXXIII, portraying the spray by two independent photographic techniques. The instantaneous pictures were taken by means of the spark-lighting apparatus while the spray envelopes shown were obtained by time exposure with reflected light.

Each figure represents the full series of nozzles, increasing in size from left to right, at one condition of air rate and fuel rate, and for one type of injection. The number beneath each picture refers to the experimental run listed in Appendix F. The plates are arranged as to type of injection and for each type, they are arranged in order of increasing air rate, and at each air rate, two plates are arranged in order of increasing fuel rate. Pictures of the spray envelope were obtained for downstream flow only because of the generally poor character of the spray for the other types of injection which would make time exposures of little constructive value.

For each individual photograph, a knowledge of what is shown is necessary to permit correct analysis. The magnification is approximately 2.8. The actual magnification can be obtained by measuring the nozzle tip in the photograph and comparing it with the actual diameter for that nozzle given in the appendix. The depth of focus is about 1.5 mm. and the center of focus is on the diameter of the fuel orifice or axis of the spray. The negatives were cut down for mounting but no vital information was lost since the nozzle tip was in the center of

RESULTS

The results are presented as a series of plates, Figures V through XXXIII, portraying the spray by two independent photographic techniques. The instantaneous pictures were taken by means of the spark-lighting apparatus while the spray envelopes shown were obtained by time exposure with reflected light.

Each figure represents the full series of nozzles, increasing in size from left to right, at one condition of air rate and fuel rate, and for one type of injection. The number beneath each picture refers to the experimental run listed in Appendix F. The plates are arranged as to type of injection and for each type, they are arranged in order of increasing air rate, and at each air rate, two plates are arranged in order of increasing fuel rate. Pictures of the spray envelope were obtained for downstream flow only because of the generally poor character of the spray for the other types of injection which would make time exposures of little constructive value.

For each individual photograph, a knowledge of what is shown is necessary to permit correct analysis. The magnification is approximately 2.8. The actual magnification can be obtained by measuring the nozzle tip in the photograph and comparing it with the actual diameter for that nozzle given in the appendix. The depth of focus is about 1.5 mm. and the center of focus is on the diameter of the fuel orifice or axis of the spray. The negatives were cut down for mounting but no vital information was lost since the nozzle tip was in the center of the chamber in all cases and the chamber walls may be reconstructed knowing the magnification. In some photos, the chamber wall shows as a black strip to the right or left and was indicated where impingement was present. The nozzle tip is shown in the prints on the top for down stream, from the left for perpendicular injection and from below for upstream injection. Out-of-focus imperfections are unavoidable, particularly at low air velocities due to fuel impingement on the optical flats.

Fuel rates of 1.08 and 3.34 grams per second and air rates of 40, 80, and 180 grams per second were chosen bearing in mind that the change in air rate is logarithmic in character and that the intermediate range might be expected to prove of greatest interest. The metric system was used here to keep numbers large enough to handle, and weight rates were used because the metering was more feasible in terms of weight.

the chamber in all cases and the chamber walls may be reconstructed knowing the magnification. In some photos, the chamber wall shows as a black strip to the right or left and was indicated where impingement was present. The nozzle tip is shown in the prints on the top for down stream, from the left for perpendicular injection and from below for upstream injection. Out-of-focus imperfections are unavoidable, particularly at low air velocities due to fuel impingement on the optical flats.

Fuel rates of 1.00 and 2.34 grams per second and air rates of 40, 80, and 160 grams per second were chosen keeping in mind that the change in air rate is logarithmic in character and that the intermediate range might be expected to prove of greatest interest. The metric system was used here to keep numbers large enough to handle, and weight rates were used because the metering was more feasible in terms of weight.

DISCUSSION OF RESULTS

There is a question as to the value of the photographs regarding their reproducibility. In all, 228 runs were made, mostly all concerned with downstream flow, and the best negative chosen for each condition. For the instantaneous pictures, no marked misrepresentation was noted in any case. However, to substantiate their value further, three pictures were taken in rapid succession for each nozzle at an air and fuel rate known to give acceptable atomization. Two of the three taken are shown in Figures XVII, XVIII, XIX, XX and XXI. They may be compared with the third, which was inserted in its proper place in the series, Figure X. The Spray Envelopes, however, are not so easily validated. The density of the negative is a function of the density and reflectability of the spray itself. At the spray cone edges, where drops are small and density is light, definition is not good in the negative and it is bettered in developing only at the expense of losing some of the edge and thus not exactly portraying the true cone. In printing negatives of varying density simultaneously, the loss of definition is constant, but the ones of lighter density suffer more in order to bring out the heavier ones. This is most readily illustrated in the pictures at low air velocities where spray density was quite light.

Two important features of the instantaneous photographs must be noted in order to understand what is actually recorded.

DISCUSSION OF RESULTS

There is a question as to the value of the photographs regarding their reproducibility. In all, 228 runs were made, mostly all concerned with downstream flow, and the best negative chosen for each condition. For the instantaneous pictures, no marked misrepresentation was noted in any case. However, to substantiate their value further, three pictures were taken in rapid succession for each nozzle at an air and fuel rate known to give acceptable atomization. Two of the three taken are shown in Figures XVII, XVIII, XIX, XX and XXI. They may be compared with the third, which was inserted in its proper place in the series, Figure X. The Spray Envelopes, however, are not so easily validated. The density of the negative is a function of the density and reflectability of the spray itself. At the spray cone edges, where drops are small and density is light, definition is not good in the negative and it is bettered in developing only at the expense of losing some of the edge and thus not exactly portraying the true cone. In printing negatives of varying density simultaneously, the loss of definition is constant, but the ones of lighter density suffer more in order to bring out the heavier ones. This is most readily illustrated in the pictures at low air velocities where spray density was quite light.

Two important features of the instantaneous photographs must be noted in order to understand what is actually recorded.

First, because the picture was not truly taken "instantaneously", though the exposure time is very small, there will be a greater ratio of large drops to small drops than actually exists, due to the fact that the smallest drops are accelerated faster and cannot be "stopped". Secondly, the exposure time limits the size of drop that can be "stopped". In order for a drop to be "stopped", it must not travel its own diameter during the time of exposure. Knowing the time of exposure to be less than 0.025 microseconds, it may be calculated that the spark will "stop" drops of size greater than 5 microns for an air velocity of 660 feet per second and 2 microns for an air velocity of 275 feet per second, and probably "stops" even smaller ones.

The nature of the equipment limits the accuracy with which conditions may be reproduced. Consequently, a representative value of fuel rate and air velocity was chosen for labelling each figure. This is an acceptable procedure for a qualitative investigation. The actual data and calculations for each run are given in Appendix F for reference.

Eastman Plus X Fine Grain film packs were used throughout, with an aperture of f 3.5. Negatives through Run 80 were developed in Eastman Microdol Developer, over-developed 100% to give maximum contrast and good grain for future enlargement. It was then realized that a more compact presentation of results would be desirable, obviating the use of enlargements, so all subsequent negatives were given normal development in Eastman D-11 Developer. It was also physically impossible to duplicate exactly the light intensity on the film when the lens

First, because the picture was not truly taken "instantaneously", though the exposure time is very small, there will be a greater ratio of large drops to small drops than actually exists, due to the fact that the smallest drops are accelerated faster and cannot be "stopped". Secondly, the exposure time limits the size of drop that can be "stopped". In order for a drop to be "stopped", it must not travel its own diameter during the time of exposure. Knowing the time of exposure to be less than 0.025 microseconds, it may be calculated that the spark will "stop" drops of size greater than 5 microns for an air velocity of 600 feet per second and 2 microns for an air velocity of 275 feet per second, and probably "stops" even smaller ones.

The nature of the equipment limits the accuracy with which conditions may be reproduced. Consequently, a representative value of fuel rate and air velocity was chosen for labelling each figure. This is an acceptable procedure for a qualitative investigation. The actual data and calculations for each run are given in Appendix I for reference.

Eastman Plus X Fine Grain film packs were used throughout, with an aperture of f 3.5. Negatives through Run 80 were developed in Eastman Microdol Developer, over-developed 100% to give maximum contrast and good grain for future enlargement. It was then realized that a more compact presentation of results would be desirable, obviating the use of enlargements, so all subsequent negatives were given normal development in Eastman D-11 Developer. It was also physically impossible to duplicate exactly the light intensity on the film when the lens arrangement was disturbed. For these reasons, the density of the instantaneous pictures was not constant in all negatives leading to non-uniform results in printing. Insufficient time prevented using a more suitable but more tedious technique of printing each negative to best results, stripping the prints in a plate and rephotographing the plate.

The following exceptions from standard conditions are noted:

1. Fig. VI - Run 79 - Nozzle tip just out of picture.
2. Fig. XXIII - Run 144 - Fuel rate 2.50 gms/sec. to prevent impingement.
3. Fig. XXV - Run 149 - Fuel rate 3.05 gms/sec. to prevent impingement.
4. Fig. XXIX - Run 91 - Tip of spray 4.00 inches above nozzle tip.
5. Fig. XXIX - Run 99 - Tip of spray 3.64 inches above nozzle tip.

It is apparent from a comparison of the Spray Envelope pictures with the instantaneous pictures, that the time exposure technique is incapable of telling the true story of atomization. In many instances, the time exposures give an illusion of a good mist formation, but the instantaneous pictures show incomplete atomization, often with fuel mass concentrations. This is easily explained by the fact that the negative receives many traces during exposure instead of recording a physical mass position. When the fuel becomes well atomized, the dispersion of drops causes a diffusion of the arrangement was disturbed. For these reasons, the density of the instantaneous pictures was not constant in all negatives leading to non-uniform results in printing. Insufficient time prevented using a more suitable but more tedious technique of printing each negative to best results, stripping the prints in a plate and rephotographing the plate.

The following exceptions from standard conditions are noted:

1. Fig. VI - Run 79 - Nozzle tip just out of picture.
2. Fig. XXIII - Run 144 - Fuel rate 2.50 gms/sec. to prevent impingement.
3. Fig. XIV - Run 143 - Fuel rate 3.05 gms/sec. to prevent impingement.
4. Fig. XXIX - Run 91 - Tip of spray 4.00 inches above nozzle tip.
5. Fig. XXXI - Run 99 - Tip of spray 3.54 inches above nozzle tip.

It is apparent from a comparison of the Spray Envelope pictures with the instantaneous pictures, that the time exposure technique is incapable of telling the true story of atomization. In many instances, the time exposures give an illusion of a good mist formation, but the instantaneous pictures show incomplete atomization, often with fuel mass concentrations. This is easily explained by the fact that the negative receives many traces during exposure instead of recording a physical mass position. When the fuel becomes well atomized, the dispersion of drops causes a diffusion of the light with the result that a fading is evident in pictures where atomization is fine and drops are well dispersed. This fading effect is small in comparison with the differences encountered in developing and printing, and, in fact, is largely dependent on them. Also, this fading effect is not uniform with increasing air or fuel rate because the film cannot differentiate between a concentration of small droplets and a solid mass concentration during long exposure. Another feature of the time exposure is that it represents the summation of positions occupied by the spray during the exposure with the consequence that spray fluctuations cause a false impression of spray volume and cone angle on the negative. It must be concluded that photographing the spray envelope with time exposure does not offer a picture valid enough for even the roughest qualitative analysis of the spray characteristics.

On the other hand, the instantaneous photographs lend themselves well to detailed analysis provided the air stream has not been disturbed sufficiently to disrupt formation of a good spray cone. An inspection of the figures indicates that Downstream flow lends itself best to analysis because of least interference from the nozzle. Only three spray characteristics can be studied with any degree of certainty: Drop Size, Dispersion, and Uniformity.

DROP SIZE: For velocities sufficient to produce acceptable atomization, no effect can be noted for increasing fuel rate or increasing orifice diameter at one air rate, and for light with the result that a fading is evident in pictures where atomization is fine and drops are well dispersed. This fading effect is small in comparison with the differences encountered in developing and printing, and, in fact, is largely dependent on them. Also, this fading effect is not uniform with increasing air or fuel rate because the film cannot differentiate between a concentration of small droplets and a solid mass concentration during long exposure. Another feature of the time exposure is that it represents the summation of positions occupied by the spray during the exposure with the consequence that spray fluctuations cause a false impression of spray volume and cone angle on the negative. It must be concluded that photographing the spray envelope with time exposure does not offer a picture valid enough for even the roughest qualitative analysis of the spray characteristics.

On the other hand, the instantaneous photographs lend themselves well to detailed analysis provided the air stream has not been disturbed sufficiently to disrupt formation of a good spray cone. An inspection of the figures indicates that Downstream flow lends itself best to analysis because of least interference from the nozzle. Only three spray characteristics can be studied with any degree of certainty: Drop Size, Dispersion, and Uniformity.

DROP SIZE: For velocities sufficient to produce acceptable atomization, no effect can be noted for increasing fuel rate or increasing orifice diameter at one air rate, and for one type of flow. At low air velocities, the velocity of the fuel is a greater percentage of the air velocity than at high, with the consequence that the change in fuel velocity imposed by change of orifice diameter or increase of fuel rate has a more noticeable effect on the relative velocity of fuel to air, and a decrease in drop size is observed for increased nozzle size and decreased fuel rate. At high air velocities, the change in relative fuel to air velocity with change in fuel rate and nozzle size is so small that the effect on drop size is not noticeable. For one fuel rate and one nozzle size, increased air velocity has a marked effect on the decrease in drop size. As the type of injection is shifted from downstream, through perpendicular to upstream, the relative velocity of fuel to air becomes greater, other variables constant, with the result that drop size decreases. The effect is more noticeable with large nozzles than with small, which leads to the conclusion that the influence of type of injection on drop size as photographed is exaggerated by the fact that there is more physical interference from the large nozzle, causing more fuel to be pulled out of the spray along the nozzle. This amounts to an appreciable decrease in fuel being atomized.

DISPERSION: Dispersion decreases with an increase in air velocity for all types of injection, due to increased stability and increased resistance to distortion of streamlinesas air velocity increases. It decreases with increased fuel rate for downstream flow, probably because of the greater stability of a more rapidly moving liquid column at the same air velocity. For perpendicular injection, the dispersion increases because one type of flow. At low air velocities, the velocity of the fuel is a greater percentage of the air velocity than at high, with the consequence that the change in fuel velocity imposed by change of orifice diameter or increase of fuel rate has a more noticeable effect on the relative velocity of fuel to air, and a decrease in drop size is observed for increased nozzle size and decreased fuel rate. At high air velocities, the change in relative fuel to air velocity with change in fuel rate and nozzle size is so small that the effect on drop size is not noticeable. For one fuel rate and one nozzle size, increased air velocity has a marked effect on the decrease in drop size. As the type of injection is shifted from downstream, through perpendicular to upstream, the relative velocity of fuel to air becomes greater, other variables constant, with the result that drop size decreases. The effect is more noticeable with large nozzles than with small, which leads to the conclusion that the influence of type of injection on drop size as photographed is exaggerated by the fact that there is more physical interference from the large nozzle, causing more fuel to be pulled out of the spray along the nozzle. This amounts to an appreciable decrease in fuel being atomized.

<u>DISPERSION</u>: Dispersion decreases with an increase in air velocity for all types of injection, due to increased stability and increased resistance to distortion of streamlines as air velocity increases. It decreases with increased fuel rate for downstream flow, probably because of the greater stability of a more rapidly moving liquid column at the same air velocity. For perpendicular injection, the dispersion increases because

the increase in fuel velocity, with increase in fuel rate and decrease in orifice size, serves only to shoot the fuel column farther across the air stream, affording more area upon which the air can work. For upstream injection, the increased fuel velocity shoots the fuel column farther upstream. The farther the fuel column goes, the more it loses its stability and becomes dispersed, thus presenting a greater area of impact to the onrushing air.

Increasing nozzle size increases dispersion for all types of injection, though the effect is not well illustrated for perpendicular injection. As nozzle size increases, the perimeter of the fuel column increases, providing more surface on which the air may act. For upstream injection, larger nozzles provide a greater area of impact to the velocity front.

UNIFORMITY: In atomization, the limit of drop size is one infinitely small, and this is approached asymptotically, with the force required to obtain it increasing in a like manner, i.e., an infinite shearing force being required to give an infinitely small drop size. When the atomizing force increases, fewer large drops will occur in relation to the number of small. Thus, with a general decrease in mean drop size, the decrease is at the expense of large drops being broken up. This amounts to saying that the variation of drop size from the mean is less with a decrease in mean drop size, and this variation is the definition of uniformity. This reasoning is confirmed by the photographs. Increased air rate gives better uniformity for all types of injection. Increased fuel rate the increase in fuel velocity, with increase in fuel rate and decrease in orifice size, serves only to shoot the fuel column farther across the air stream, affording more area upon which the air can work. For upstream injection, the increased fuel velocity shoots the fuel column farther upstream. The farther the fuel column goes, the more it loses its stability and becomes dispersed, thus presenting a greater area of impact to the onrushing air.

Increasing nozzle size increases dispersion for all types of injection, though the effect is not well illustrated for perpendicular injection. As nozzle size increases, the perimeter of the fuel column increases, providing more surface on which the air may act. For upstream injection, larger nozzles provide a greater area of impact to the velocity front.

UNIFORMITY: In atomization, the limit of drop size is one infinitely small, and this is approached asymptotically, with the force required to obtain it increasing in a like manner, i.e., an infinite shearing force being required to give an infinitely small drop size. When the atomizing force increases, fewer large drops will occur in relation to the number of small. Thus, with a general decrease in mean drop size, the decrease is at the expense of large drops being broken up. This amounts to saying that the variation of drop size from the mean is less with a decrease in mean drop size, and this variation is the definition of uniformity. This reasoning is confirmed by the photographs. Increased air rate gives better uniformity for all types of injection. Increased fuel rate decreases the uniformity. The effect of nozzle size is not marked except in upstream flow where the same illusion occurs as explained in the discussion of drop size regarding the amount of fuel drawn out of the column by the larger nozzle.

In line with these observations, an attempt was made to apply the formulation of Nukiyama and Tanisawa (15) in order to predict the effect of the variables on Mean Drop Size. These investigators tested a small nozzle, using liquid fuels injected into the throat of a venturi atomizer with air as the atomizing agent. From their tests they determined that:

$$D_m = \frac{585\sqrt{\sigma}}{V\sqrt{\rho}} + 597\left(\frac{\mu}{\sqrt{\rho\sigma}}\right)^{0.45}\left(\frac{1000\,Q_f}{Q_a}\right)^{1.5} \qquad [1]$$

where:

D_m = Volume-surface mean diameter in microns.

V = Relative velocity of air to liquid - meters/second.

σ = Surface tension of liquid - dynes/cm.

ρ = Density of liquid - grams/cc.

μ = Viscosity of liquid - dynes-sec./sq.cm.

Q_f = Volume rate of liquid - cc./sec.

Q_a = Volume rate of air - cc./sec.

They found no effect on drop size from changing the size of venturi, within small limits. Lewis and Edwards (17) have also shown that the equation gives good results for venturis of any size. In particular, they tested perpendicular injection from a small nozzle into the throat of a relatively large venturi. This constitutes point injection into a reasonably uniform air stream, and they found that equation (1) still held.

decreases the uniformity. The effect of nozzle size is not marked except in upstream flow where the same illusion occurs as explained in the discussion of drop size regarding the amount of fuel drawn out of the column by the larger nozzle.

In line with these observations, an attempt was made to apply the formulation of Nukiyama and Tanasawa (15) in order to predict the effect of the variables on Mean Drop Size. These investigators tested a small nozzle, using liquid fuels injected into the throat of a venturi atomizer with air as the atomizing agent. From their tests they determined that:

$$D_{vm} = \frac{585\sqrt{\sigma}}{V\sqrt{\rho}} + 597\left(\frac{\mu}{\sqrt{\sigma\rho}}\right)^{0.45}\left(\frac{1000\,Q_f}{Q_a}\right)^{1.5} \qquad [1]$$

where:

D_{vm} = Volume-surface mean diameter in microns.

V = Relative velocity of air to liquid - meters/second.

σ = Surface tension of liquid - dynes/cm.

ρ = Density of liquid - grams/cc.

μ = viscosity of liquid - dynes-sec./sq.cm.

Q_f = Volume rate of liquid - cc./sec.

Q_a = Volume rate of air - cc./sec.

They found no effect on drop size from changing the size of venturi, within small limits. Lewis and Edwards (17) have also shown that the equation gives good results for venturis of any size. In particular, they tested perpendicular injection from a small nozzle into the throat of a relatively large venturi. This constitutes point injection into a reasonably uniform air stream, and they found that equation (1) still held.

TABLE I

For Diesel Oil: $Dm = \frac{3220}{V} + 41.5 \left(\frac{1000\ Q_f}{Q_a}\right)^{1.5}$

Fig.	Run No.	Nozzle No.	Va	Vf	V	$\frac{3220}{V}$	Q_f	Q_a	$\left(\frac{1000 Q_f}{Q_a}\right)^{1.5}$	Dm
					DOWNSTREAM					
VI	79	5	42.7	5.0	37.7	85.5	1.33	27400	.47	86.0
VI	77	1	45.8	.2	45.6	70.6	1.26	29400	.37	71.0
VIII	161	1	41.1	.7	40.4	79.8	3.95	26400	2.4	82.2
X	178	5	83.0	4.9	78.1	41.2	1.31	153600	.03	41.2
X	171	4	80.5	2.2	78.3	41.1	1.30	51900	.16	41.3
X	167	3	82.6	.82	81.8	39.4	1.28	53400	.15	39.6
X	152	2	82.6	.36	82.2	39.2	1.31	53400	.16	39.3
X	158	1	80.0	.24	79.8	40.4	1.31	51400	.16	40.6
XII	181	5	83.0	15.0	68.0	47.4	4.04	53500	.87	48.3
XII	39	4	86.5	7.0	79.5	40.5	4.10	55800	.84	41.3
XII	26	3	84.6	2.6	82.0	39.3	4.04	54600	.84	40.1
XII	51	2	87.1	1.1	86.0	37.5	3.93	56100	.75	38.3
XII	75	1	84.8	.7	84.1	38.3	4.03	54800	.84	39.1
XIV	182	5	199	5.1	194.1	16.6	1.29	128500	.04	16.6
XIV	157	1	201	.24	201.0	16.0	1.33	130000	.04	16.0
XVI	17	5	203	15.1	188.0	17.2	4.06	131000	.23	17.4
XVI	74	1	204	.73	203.3	15.9	4.03	131300	.23	16.1
					PERPENDICULAR					
XXVI	145	5	196	4.8	196.0	16.4	1.30	120000	.04	16.4
XXVII	146	5	199	15.1	199.0	16.2	4.06	128500	.23	16.4
					UPSTREAM					
XXXII	85	5	216	4.3	220.0	14.6	.87	139000	.01	14.6
XXXIII	86	5	202	15.0	217.0	14.8	4.04	130000	.23	15.0

Note: Nozzle size decreases from #1 to #5. Dimensions given in Appendix "D".

TABLE I

For Diesel Oil: $D_m = \frac{3220}{V} + 41.5 \left(\frac{1000\, G_f}{G_a}\right)^{1.5}$

Fig.	Run No.	Nozzle No.	V_a	V_f	V	$\frac{3220}{V}$	G_f	G_a	$\left(\frac{1000 G_f}{G_a}\right)^{1.5}$	D_m
					DOWNSTREAM					
VI	79	5	42.7	5.0	37.7	85.5	1.33	27400	.47	86.0
VI	77	1	45.8	.2	45.6	70.6	1.26	29400	.37	71.0
VIII	161	1	41.1	.7	40.4	79.8	3.95	26400	2.4	82.2
X	178	5	83.0	4.9	78.1	41.2	1.31	153600	.03	41.2
X	171	4	80.5	2.2	78.3	41.1	1.30	51900	.16	41.3
X	167	3	82.6	.82	81.8	39.4	1.28	53400	.15	39.6
X	152	2	82.6	.36	82.2	39.2	1.31	53400	.15	39.3
X	159	1	80.0	.24	79.8	40.4	1.31	51400	.16	40.6
XII	181	5	83.0	15.0	68.0	47.4	4.04	53500	.87	48.3
XII	39	4	86.5	7.0	79.5	40.5	4.10	55800	.84	41.3
XII	26	3	84.6	2.6	82.0	39.3	4.04	54600	.84	40.1
XII	51	2	87.1	1.1	86.0	37.5	3.93	56100	.75	38.3
XII	75	1	84.8	.7	84.1	38.3	4.03	54800	.84	39.1
XIV	182	5	199	5.1	194.1	16.6	1.29	128500	.04	16.6
XIV	157	1	201	.24	201.0	16.0	1.33	130000	.04	16.0
XVI	17	5	203	15.1	188.0	17.2	4.06	131000	.23	17.4
XVI	74	1	204	.73	203.3	15.9	4.03	131300	.23	16.1
					PERPENDICULAR					
XXVI	145	5	196	4.8	196.0	16.4	1.30	120000	.04	16.4
XXVII	146	5	199	15.1	199.0	16.2	4.06	128500	.23	16.4
					UPSTREAM					
XXXII	65	5	216	4.3	220.0	14.6	.87	139000	.01	14.6
XXXIII	66	5	202	15.0	217.0	14.8	4.04	130000	.23	15.0

Note: Nozzle size decreases from #1 to #5. Dimensions given in Appendix "D".

Table I includes the calculations for sufficient pertinent runs to provide a basis for correlation.

The conclusions drawn from this analysis generally agree with those observed in the photographs. The variables investigated in this thesis affect the formula in the following ways: (a) Increase of nozzle size decreases the fuel velocity, thus affecting the relative velocity V; (b) Increased fuel rate increases the fuel velocity, thus affecting relative velocity, and increasing Qf; (c) Increased air rate increases the relative velocity V and increases Qa; (d) Type of injection affects relative velocity V - fuel and air velocities being subtracted for downstream, added for upstream, and fuel velocity being neglected for perpendicular injection. The general observation first made is that the change in mean drop size due to nozzle size, fuel rate and type of injection at air velocities sufficient to give acceptable atomization is of the same order of magnitude as the experimental error involved in this thesis. The predicted effect on mean drop size from equation (1) is most notable at low air velocity for nozzle size and fuel rate, and most apparent for type of injection at high fuel rates, as previously explained. The change in drop diameter at higher air velocities is sufficiently small, with all the studied variables except air velocity itself, to escape detection by macroscopic examination of the photographs. The variables are all significant at low air velocities, but this does not contribute much to the knowledge of atomization as regards its application to the proper combustion of fuels, since atomization is not acceptable. The

Table I includes the calculations for sufficient pertinent runs to provide a basis for correlation.

The conclusions drawn from this analysis generally agree with those observed in the photographs. The variables investigated in this thesis affect the formula in the following ways: (a) Increase of nozzle size decreases the fuel velocity, thus affecting the relative velocity V; (b) Increased fuel rate increases the fuel velocity, thus affecting relative velocity, and increasing Q_f; (c) Increased air rate increases the relative velocity V and increases Q_a; (d) Type of injection affects relative velocity V - fuel and air velocities being subtracted for downstream, added for upstream, and fuel velocity being neglected for perpendicular injection. The general observation first made is that the change in mean drop size due to nozzle size, fuel rate and type of injection at air velocities sufficient to give acceptable atomization is of the same order of magnitude as the experimental error involved in this thesis. The predicted effect on mean drop size from equation (1) is most notable at low air velocity for nozzle size and fuel rate, and most apparent for type of injection at high fuel rates, as previously explained. The change in drop diameter at higher air velocities is sufficiently small, with all the studied variables except air velocity itself, to escape detection by macroscopic examination of the photographs. The variables are all significant at low air velocities, but this does not contribute much to the knowledge of atomization as regards its application to the proper combustion of fuels, since atomization is not acceptable. The correlation does show that the formula is correct as to general trend, but its validity has been more comprehensively established by other investigators.

The photographs afford a good comparison of the types of injection and the advantages and disadvantages offered by each. The effects of each on the spray characteristics have been previously explained. A consideration of other features is also feasible. It is seen that streamlining that portion of the nozzle that extends into the air stream is desirable for downstream flow, and a definite necessity for the other types. The flow might be expected to be more asymmetrical for downstream injection than is indicated by the photographs, and probably would be in a less restricted gas duct where streamlines would have more freedom to distort laterally. Nozzle size in the range tested does not seem to be an important factor with downstream flow, but it is quite important with perpendicular and upstream injection. For the perpendicular type, the large nozzles form a definite low pressure area on the downstream side, although the tapered tip did prevent fuel from running back along the nozzle (a condition experienced by Robillard with the blunt tip). In upstream flow, general atomization was very poor because the fuel collected on all exposed portions of the nozzle and was blown off in large droplets. Also, from the combustion standpoint, it does not seem possible that a nozzle would stand up well with the flame enveloping it. In summary, perpendicular and upstream injection do not offer enough advantage in atomicorrelation does show that the formula is correct as to general trend, but its validity has been more comprehensively established by other investigators.

The photographs afford a good comparison of the types of injection and the advantages and disadvantages offered by each. The effects of each on the spray characteristics have been previously explained. A consideration of other features is also feasible. It is seen that streamlining that portion of the nozzle that extends into the air stream is desirable for downstream flow, and a definite necessity for the other types. The flow might be expected to be more asymmetrical for downstream injection than is indicated by the photographs, and probably would be in a less restricted gas duct where streamlines would have more freedom to distort laterally. Nozzle size in the range tested does not seem to be an important factor with downstream flow, but it is quite important with perpendicular and upstream injection. For the perpendicular type, the large nozzles form a definite low pressure area on the downstream side, although the tapered tip did prevent fuel from running back along the nozzle (a condition experienced by Hoblinard with the blunt tip). In upstream flow, general atomization was very poor because the fuel collected on all exposed portions of the nozzle and was blown off in large droplets. Also, from the combustion standpoint, it does not seem possible that a nozzle would stand up well with the flame enveloping it. In summary, perpendicular and upstream injection do not offer enough advantage in atomization to counterbalance the inherent disadvantages due to interference of the nozzle. Perpendicular injection does offer the easiest means of nozzle replacement, however.

The instantaneous photographs, particularly those of downstream flow, illustrate nicely the mechanism of atomization and are in good agreement with the theories expounded by Castleman (8), Rayleigh (10), and Haenlein (18), discussed in Appendix "B". It is not the purpose of this thesis to elaborate on this agreement, but attention should be called to certain points pertaining to the effect of nozzle size.

At the same fuel rate and air rate, atomization starts sooner but takes longer for completion with the large nozzle than with the small. It starts sooner because of the greater relative velocity, and takes longer for completion because of the greater stability of a fuel column of greater diameter. The fuel column from the small nozzle shatters as soon as it starts to atomize. These facts are more evident at the lowest air velocity. At high air velocities, the effect is small but still noticeable.

The mechanics of atomization are illustrated by observing the principal action of surface tension at low air velocities and the combined action of surface tension and ligament formation by shearing action at high air velocities. No evidence of the action of turbulence in the fuel column can be observed because the highest Reynolds' Number encountered was 220.

Other observations made agree with the literature in that atomization occurs closer to the orifice with increasing air zation to counterbalance the inherent disadvantages due to interference of the nozzle. Perpendicular injection does offer the easiest means of nozzle replacement, however.

The instantaneous photographs, particularly those of downstream flow, illustrate nicely the mechanism of atomization and are in good agreement with the theories expounded by Castleman (3), Rayleigh (10), and Scheubel (19), discussed in Appendix "B". It is not the purpose of this thesis to elaborate on this agreement, but attention should be called to certain points pertaining to the effect of nozzle size.

At the same fuel rate and air rate, atomization starts sooner but takes longer for completion with the large nozzle than with the small. It starts sooner because of the greater relative velocity, and takes longer for completion because of the greater stability of a fuel column of greater diameter. The fuel column from the small nozzle shatters as soon as it starts to atomize. These facts are more evident at the lowest air velocity. At high air velocities, the effect is small but still noticeable.

The mechanics of atomization are illustrated by observing the principal action of surface tension at low air velocities and the combined action of surface tension and ligament formation by shearing action at high air velocities. No evidence of the action of turbulence in the fuel column can be observed because the highest Reynolds' Number encountered was 220.

Other observations made agree with the literature in that atomization occurs closer to the orifice with increasing air velocity, and tend to agree with Scheubel and Sauter (1) in that ligaments cannot be observed above relative velocities of 10,000 - 12,000 cm/sec. It is further noted that atomization occurs closer to the orifice, with increasing orifice size.

CONCLUSIONS

From the observations and discussion it may be concluded that:

1. Spark photography affords a good representation of the degree of atomization and general spray characteristics, and that the results so obtained are reproducible.
2. Correct analysis of the atomization of a fluid cannot be made from relatively long exposure pictures of the spray.
3. With increasing orifice diameter:
   - (a) No appreciable effect is noted on drop size at air velocities sufficient to give acceptable atomization. At low air velocities, drop size decreases.
   - (b) Dispersion increases.
   - (c) Uniformity not materially affected.
4. With increased air velocity:
   - (a) Drop size decreases.
   - (b) Dispersion decreases.
   - (c) Uniformity increases.
5. With increased fuel rate:
   - (a) No appreciable effect on drop size at air velocities sufficient to give acceptable atomization. At low air velocities, drop size increases.

CONCLUSIONS

From the observations and discussion it may be concluded that:

1. Spark photography affords a good representation of the degree of atomization and general spray characteristics, and that the results so obtained are reproducible.
2. Correct analysis of the atomization of a fluid cannot be made from relatively long exposure pictures of the spray.
3. With increasing orifice diameter:
   (a) No appreciable effect is noted on drop size at air velocities sufficient to give acceptable atomization. At low air velocities, drop size decreases.
   (b) Dispersion increases.
   (c) Uniformity not materially affected.
4. With increased air velocity:
   (a) Drop size decreases.
   (b) Dispersion decreases.
   (c) Uniformity increases.
5. With increased fuel rate:
   (a) No appreciable effect on drop size at air velocities sufficient to give acceptable atomization. At low air velocities, drop size increases.

(b) Dispersion decreases for downstream injection, and increases for perpendicular and upstream injection.

(c) Uniformity decreases.

6. For type of injection:

   (a) Spray characteristics are not materially affected.

   (b) Perpendicular and upstream injection have serious nozzle design problems, with large nozzles showing the greatest disadvantages.

7. Within the limits tested, air velocity was the only variable that materially affected the fineness of atomization.

8. From all considerations; downstream injection with large nozzles offers most to proper and complete atomization.

(b) Dispersion decreases for downstream injection, and increases for perpendicular and upstream injection.

(c) Uniformity decreases.

6. For type of injection:

(a) Spray characteristics are not materially affected.

(b) Perpendicular and upstream injection have serious nozzle design problems, with large nozzles showing the greatest disadvantages.

7. Within the limits tested, air velocity was the only variable that materially affected the fineness of atomization.

8. From all considerations; downstream injection with large nozzles offers most to proper and complete atomization.

RECOMMENDATIONS

1. An attempt be made with this apparatus to atomize Bunker "C" fuel oil under carefully controlled conditions to determine the character of atomization and what air velocities are necessary for acceptable spray formation.
2. An investigation into the effect of orifice perimeter/area ratio on atomization might prove of value.
3. With the chamber redesigned to permit good side lighting, and using a much shorter exposure time and smaller lens aperture, it might be possible to correlate quantitatively cone angle with nozzle size and other variables.
4. The effect of preheat on highly viscous fuels could be investigated on this equipment.
5. Specific nozzle designs could be analyzed with this apparatus. This is particularly true for attempts to improve perpendicular injection.
6. If the apparatus is to be used for further investigation, the chamber assembly could be further improved to prevent air leaks by assuring positive contact between glass and metal walls. This could be done by drilling countersunk holes in the glass every inch along its length next to both sides and using fine thread screws into tapped holes in the metal walls. A stop valve should also be placed in the exhaust line before it joins the by-pass to permit removal of the chamber without shutting off the air compressor. Also, a simple but efficient separator should be installed on the exhaust line if heavy liquids are to be used.

RECOMMENDATIONS

1. An attempt be made with this apparatus to atomize Bunker "C" fuel oil under carefully controlled conditions to determine the character of atomization and what air velocities are necessary for acceptable spray formation.
2. An investigation into the effect of orifice perimeter/area ratio on atomization might prove of value.
3. With the chamber redesigned to permit good side lighting, and using a much shorter exposure time and smaller lens aperture, it might be possible to correlate quantitatively cone angle with nozzle size and other variables.
4. The effect of preheat on highly viscous fuels could be investigated on this equipment.
5. Specific nozzle designs could be analyzed with this apparatus. This is particularly true for attempts to improve perpendicular injection.
6. If the apparatus is to be used for further investigation, the chamber assembly could be further improved to prevent air leaks by assuring positive contact between glass and metal walls. This could be done by drilling countersunk holes in the glass every inch along its length next to both sides and using fine thread screws into tapped holes in the metal walls. A stop valve should also be placed in the exhaust line before it joins the by-pass to permit removal of the chamber without shutting off the air compressor. Also, a simple but efficient separator should be installed on the exhaust line if heavy liquids are to be used.

DOWNSTREAM INJECTION

190 197 203 228 211

FIG. V Fuel 1.08 gms./sec.
Air 140 ft./sec.

79 175 170 53 77

FIG. VI Fuel 1.08 gms./sec.
Air 140 ft./sec.

191 198 204 206 212

FIG. VII Fuel 3.34 gms./sec.
Air 140 ft./sec.

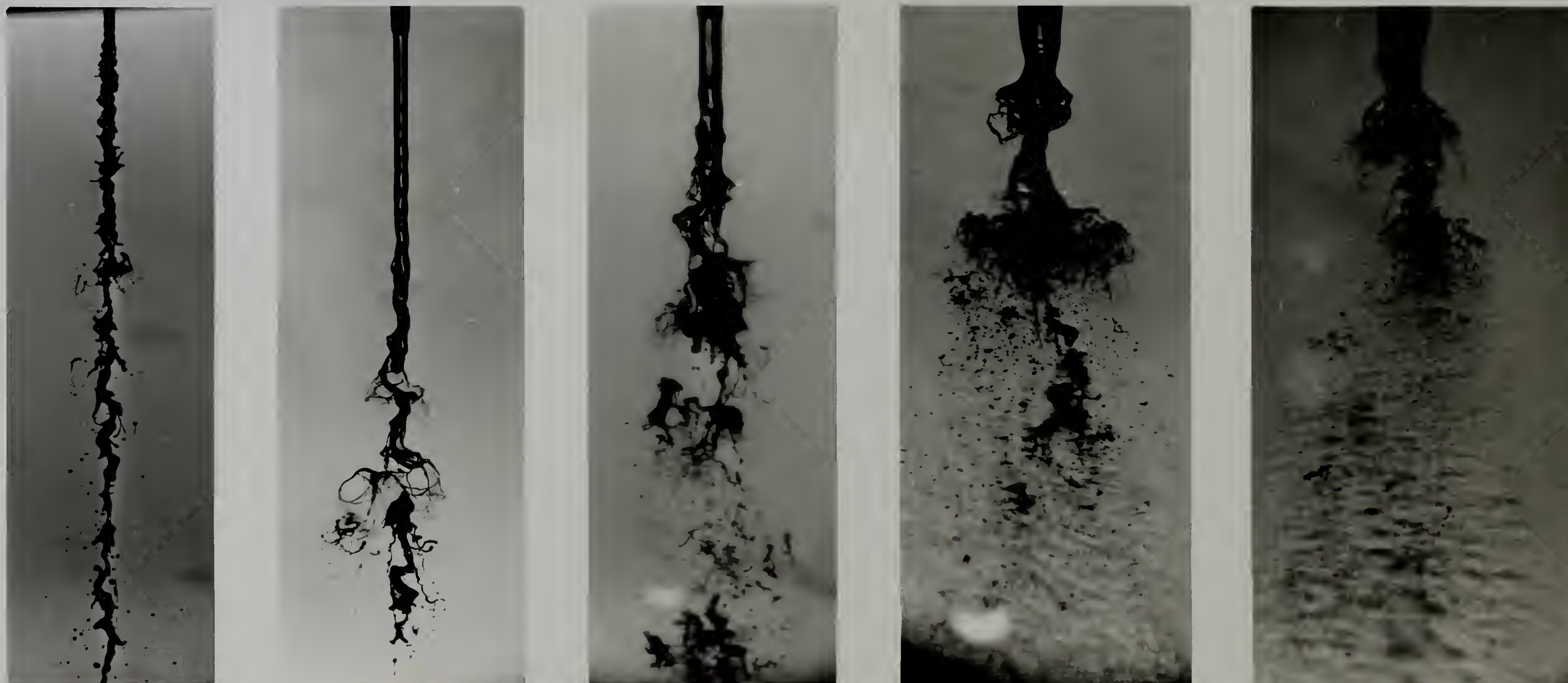

80 177 29 54 161

FIG. VIII Fuel 3.34 gms./sec.
Air 140 ft./sec.

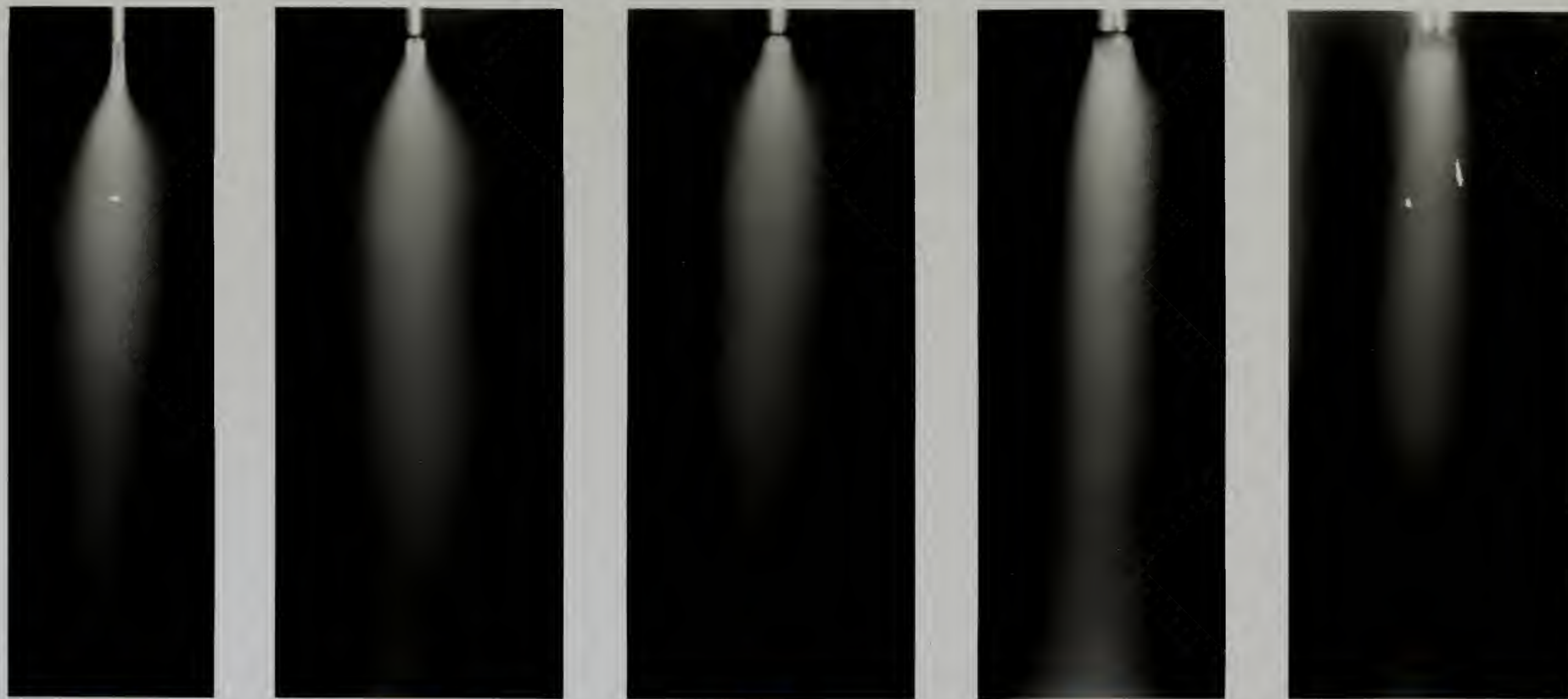

184 192 201 207 195

FIG. IX Fuel 1.08 gms./sec.
Air 275 ft./sec.

176 171 167 152 158

FIG. X Fuel 1.08 gms./sec.
Air 275 ft./sec.

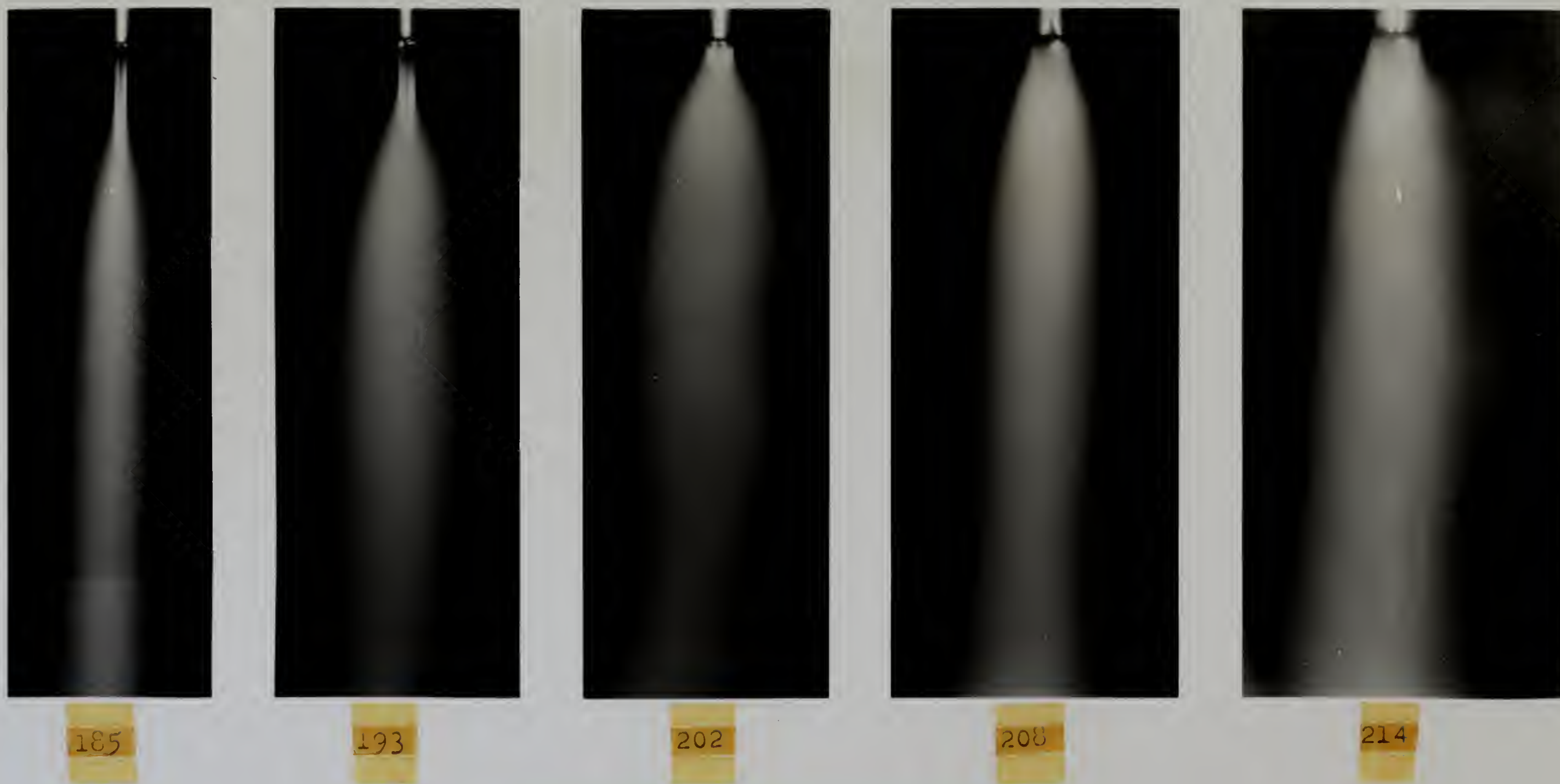

FIG. XI Fuel 3.34 gms./sec.
Air 275 ft./sec.

181 39 26 51 75

FIG. XII Fuel 3.34 gms./sec.
Air 275 ft./sec.

188 194 199 210 215

FIG. XIII Fuel 1.08 gms./sec.
Air 660 ft./sec.

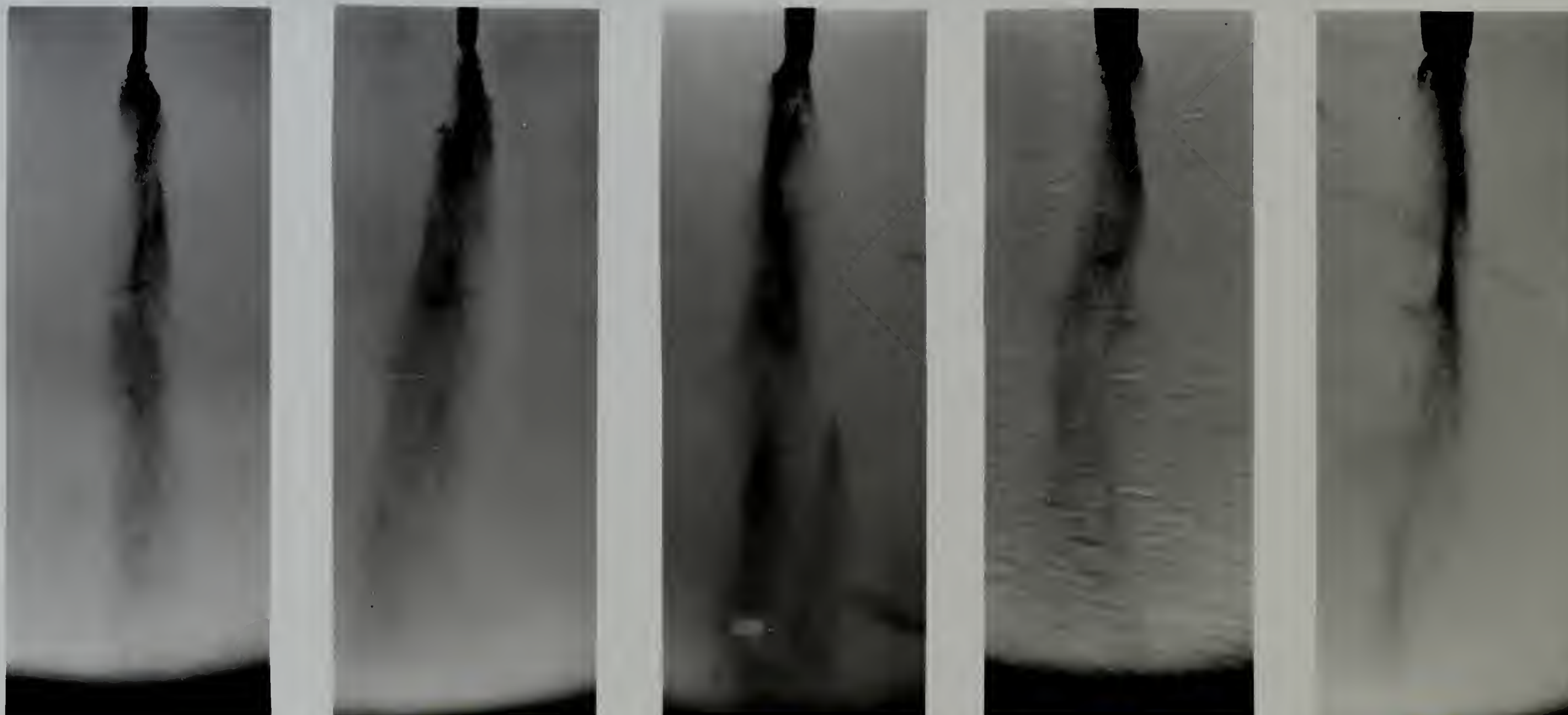

182 174 34 155 157

FIG. XIV Fuel 1.08 gms./sec.
Air 660 ft./sec.

186

195

200

209

216

FIG. XV Fuel 3.34 gms./sec.
Air 660 ft./sec.

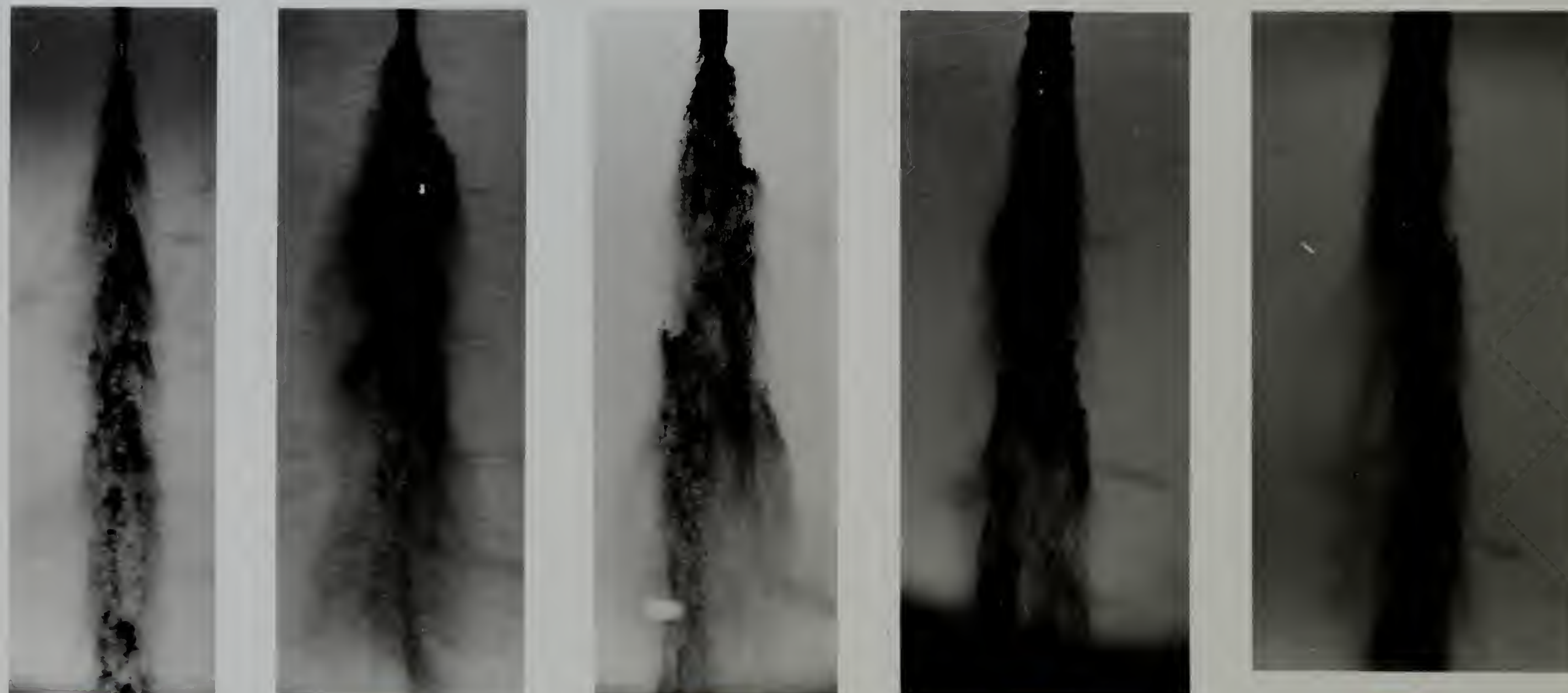

17 40 25 50 74

FIG. XVI Fuel 3.34 gms./sec.
Air 660 ft./sec.

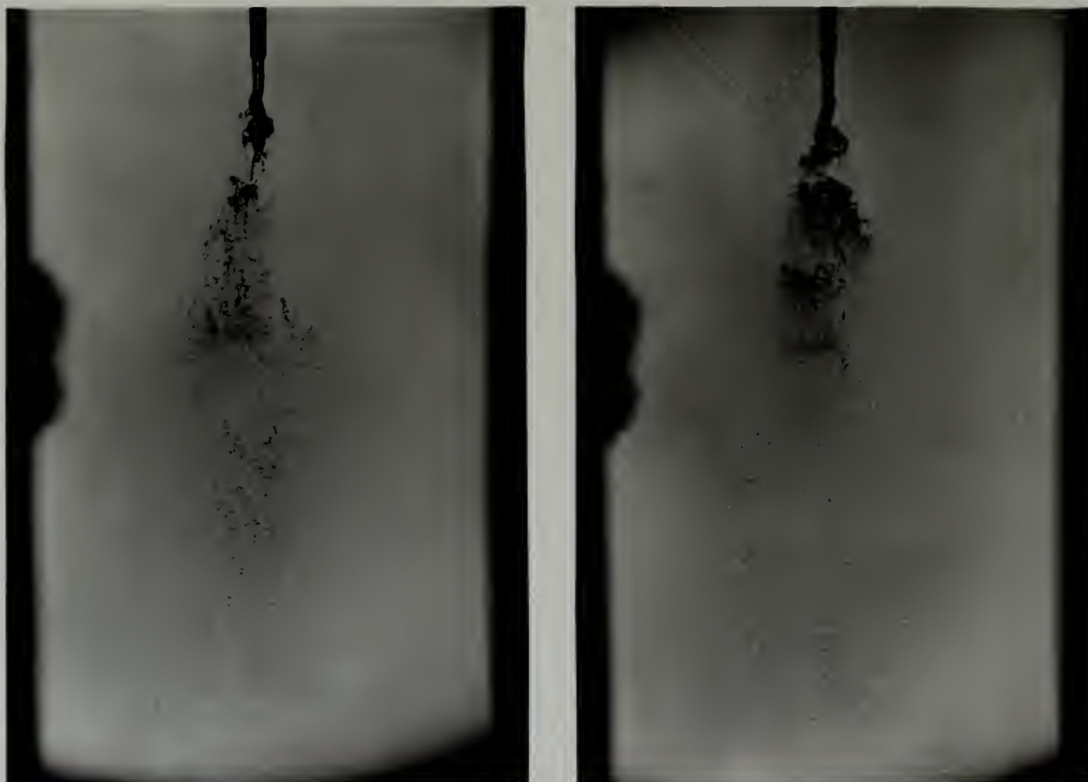

179 180

FIG. XVII Fuel 1.08 gms./sec.
Air 275 ft./sec.

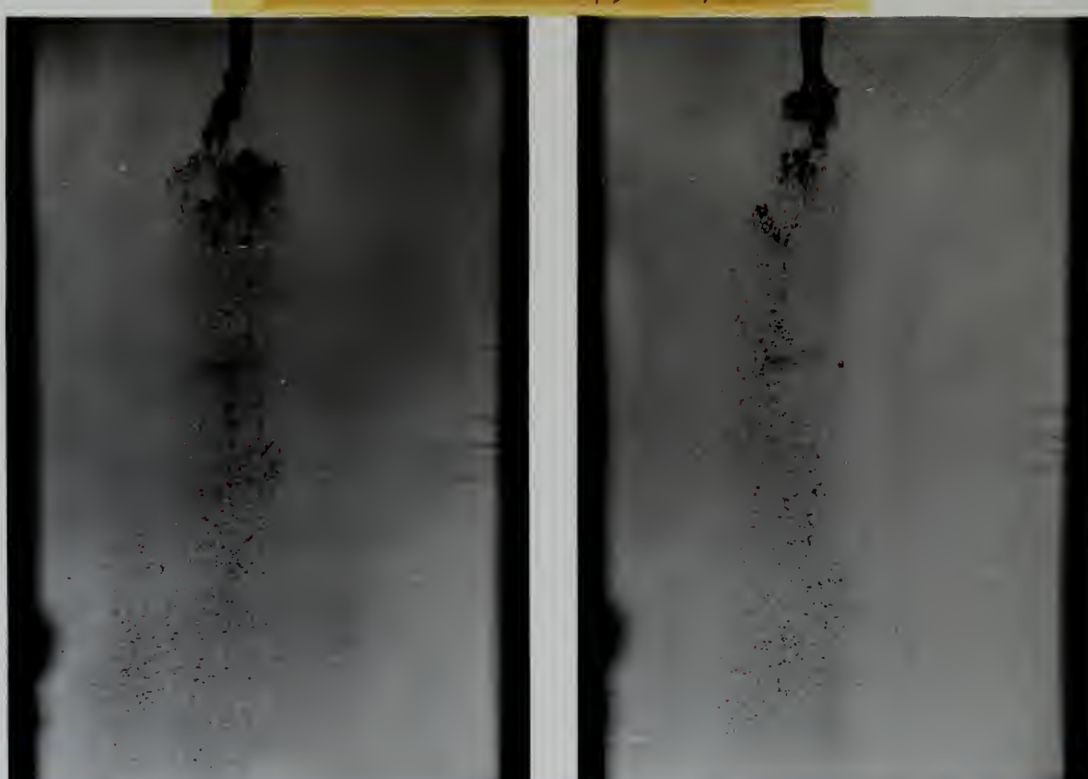

172 173

FIG. XVIII Fuel 1.08 gms./sec.
Air 275 ft./sec.

168 169

FIG. XIX Fuel 1.08 gms./sec.
Air 275 ft./sec.

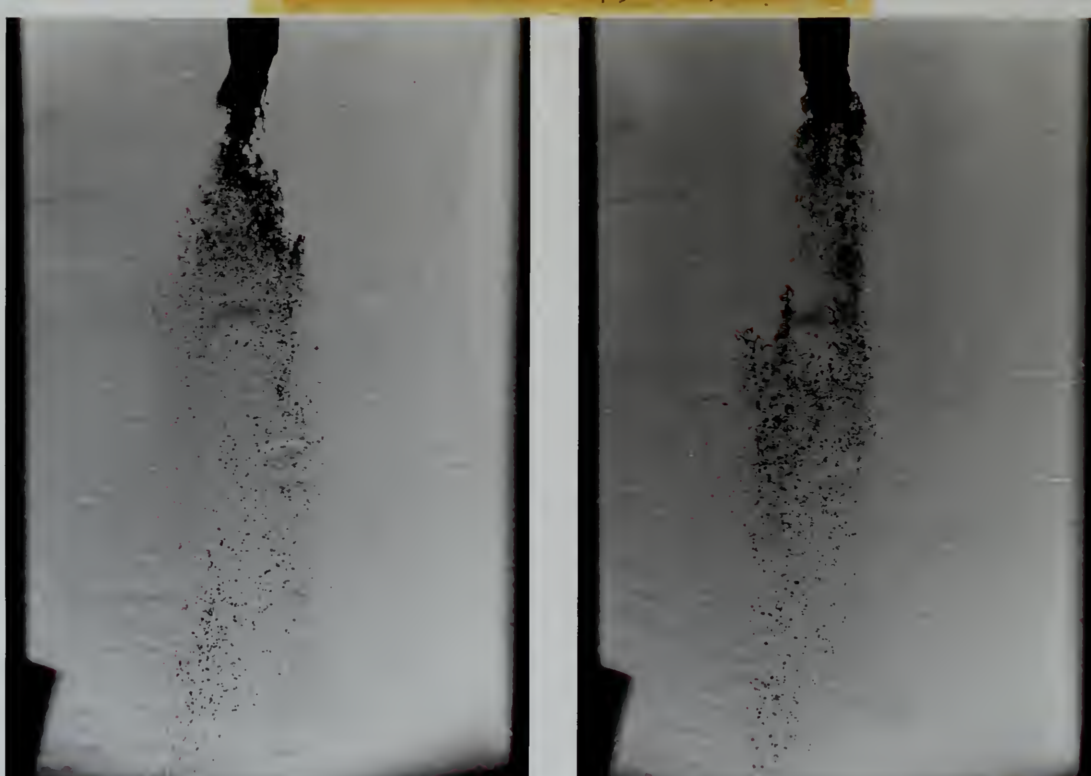

153 154

FIG. XX Fuel 1.08 gms./sec.
Air 275 ft./sec.

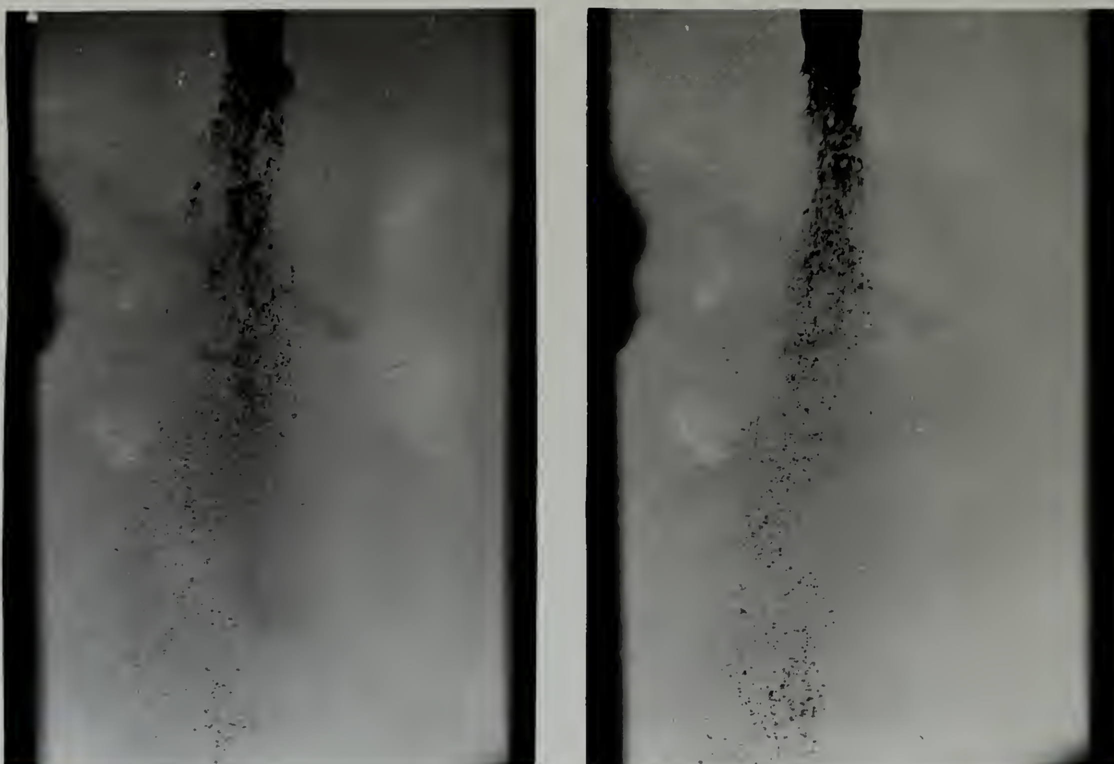

159 160

FIG. XXI Fuel 1.08gms./sec.
Air 275 ft./sec.

PERPENDICULAR INJECTION

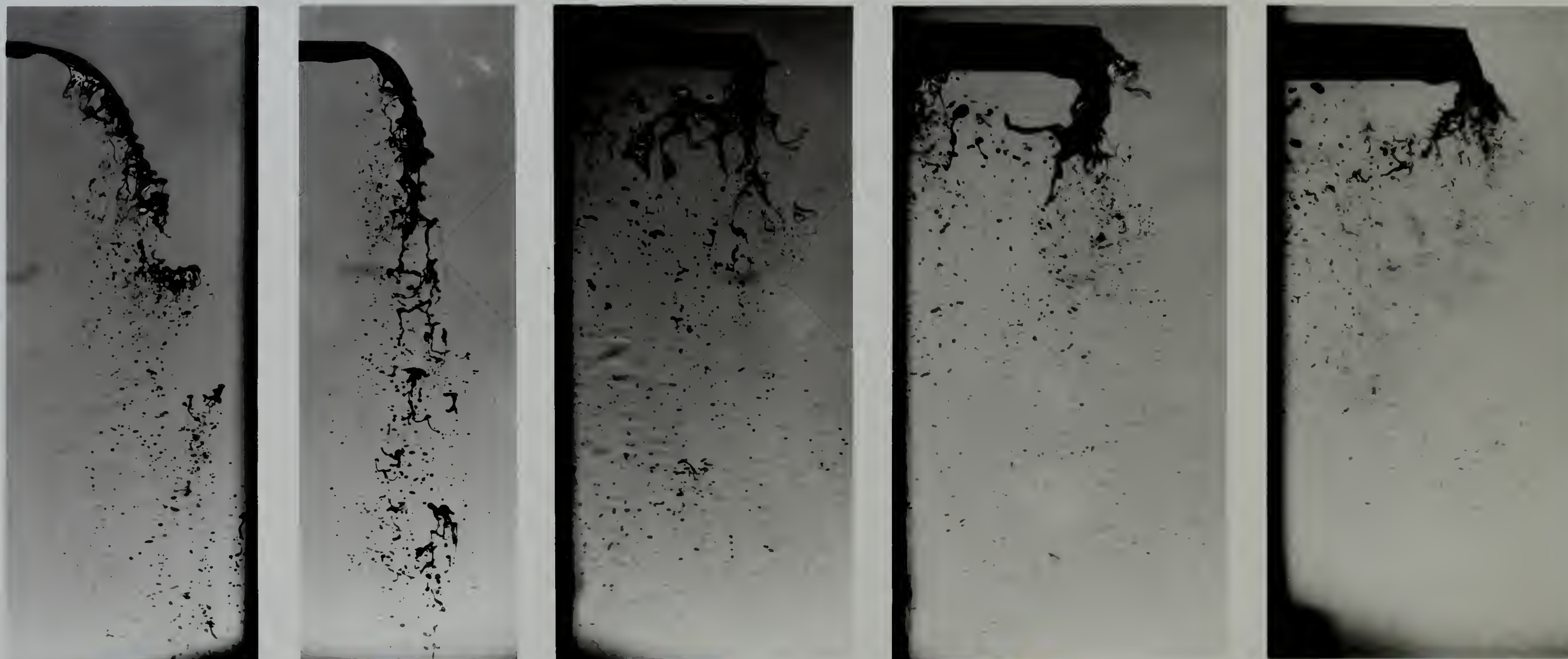

150 143 137 131 125

FIG. XXII Fuel 1.08 gms./sec.
Air 140 ft./sec.

FIG. XXIII Fuel 3.34 gms./sec.
Air 140 ft/sec.

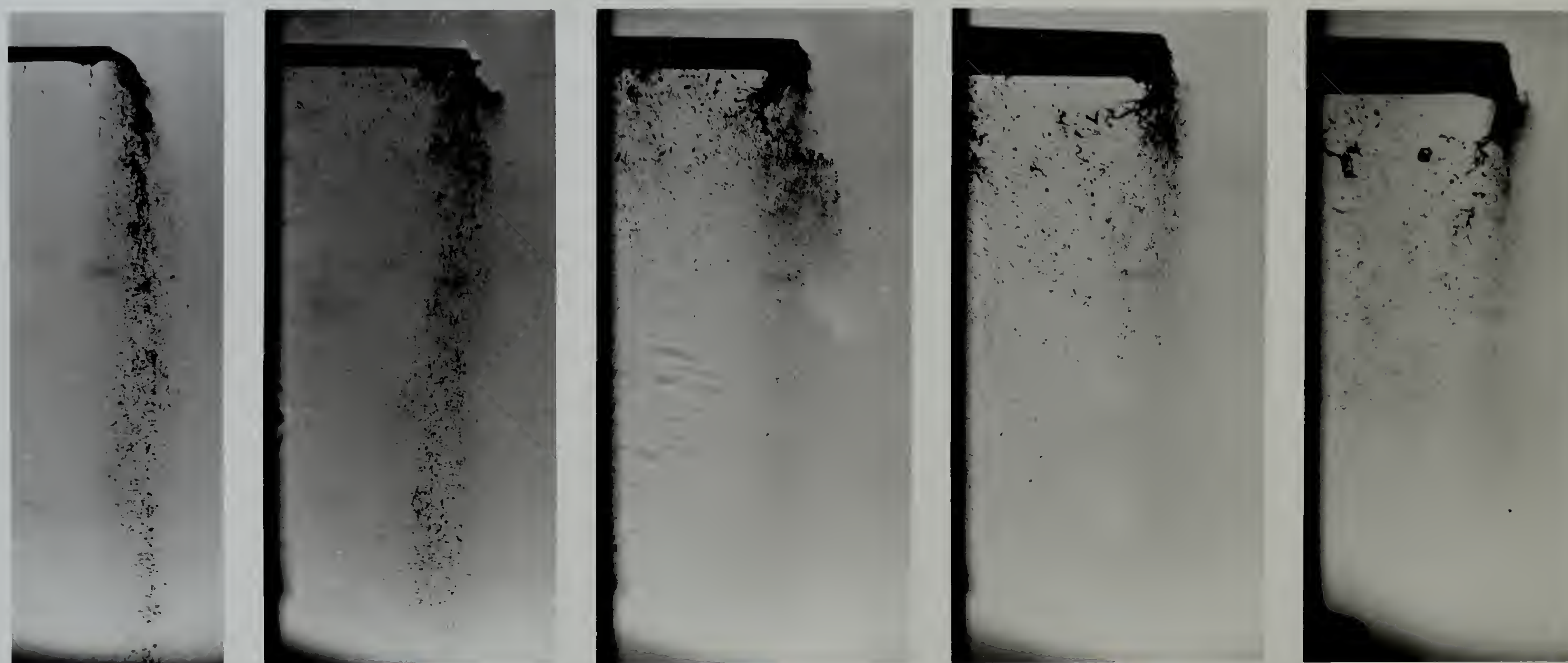

148 141 135 129 123

FIG. XXIV Fuel 1.08 gms./sec.
Air 275 ft./sec.

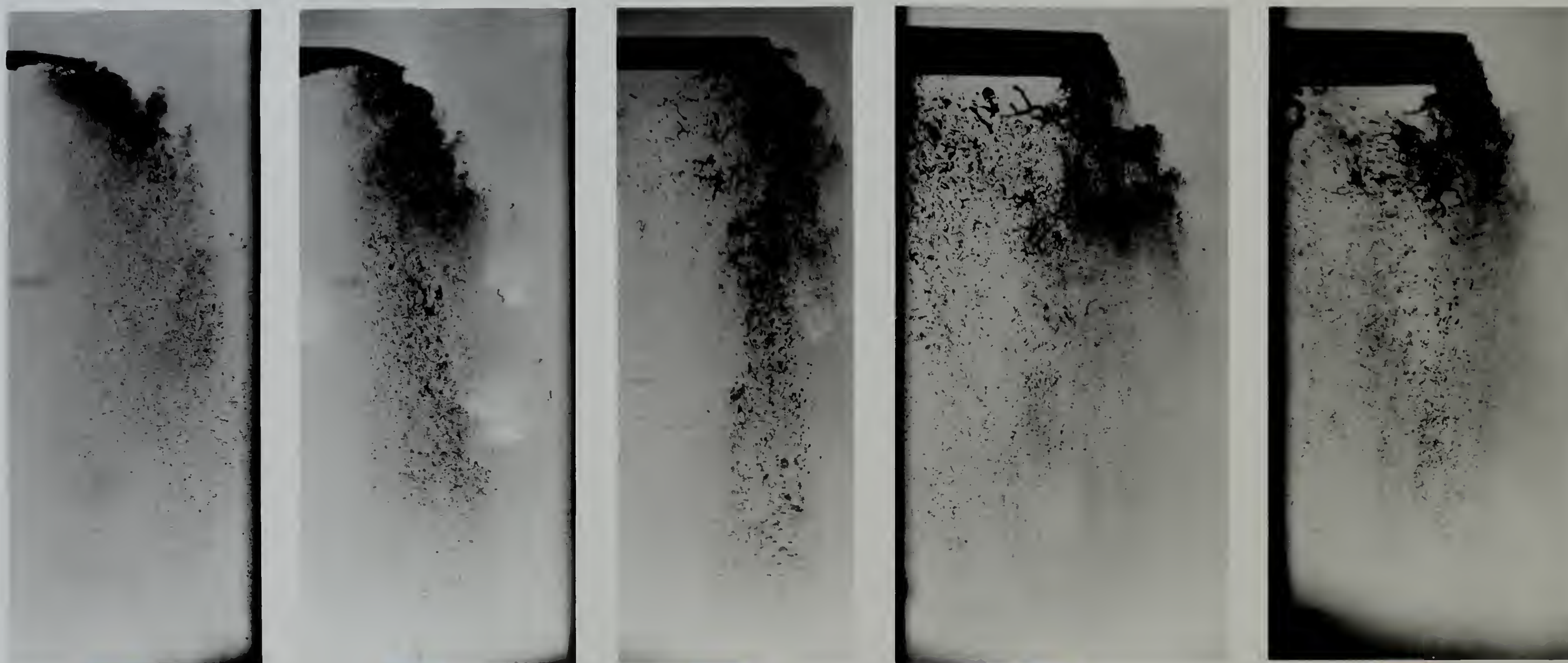

149 142 136 130 124

FIG. XXV Fuel 3.34 gms./sec.
Air 275 ft./sec.

145

220

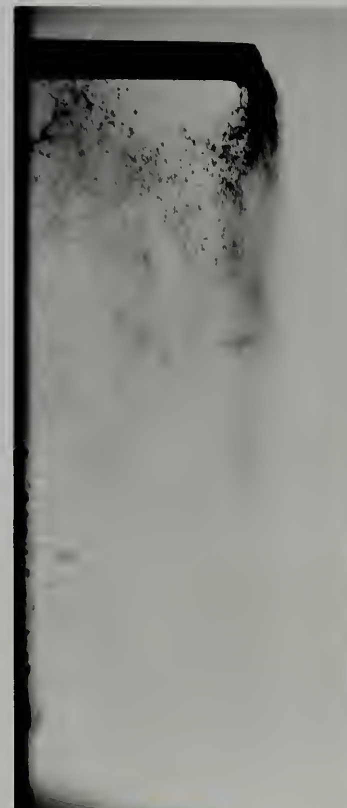

133

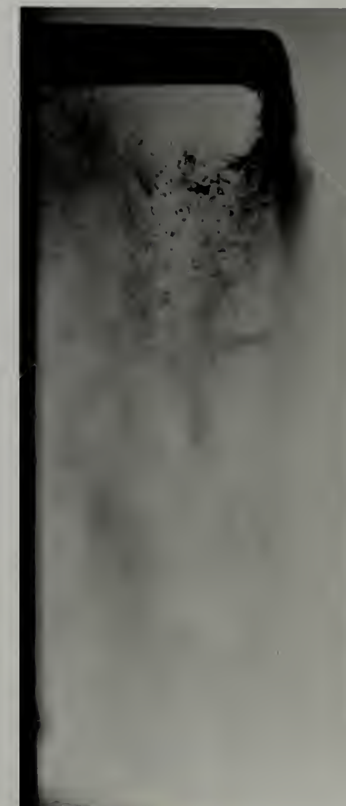

127

121

FIG. XXVI Fuel 1.08 gms./sec.
Air 660 ft/sec.

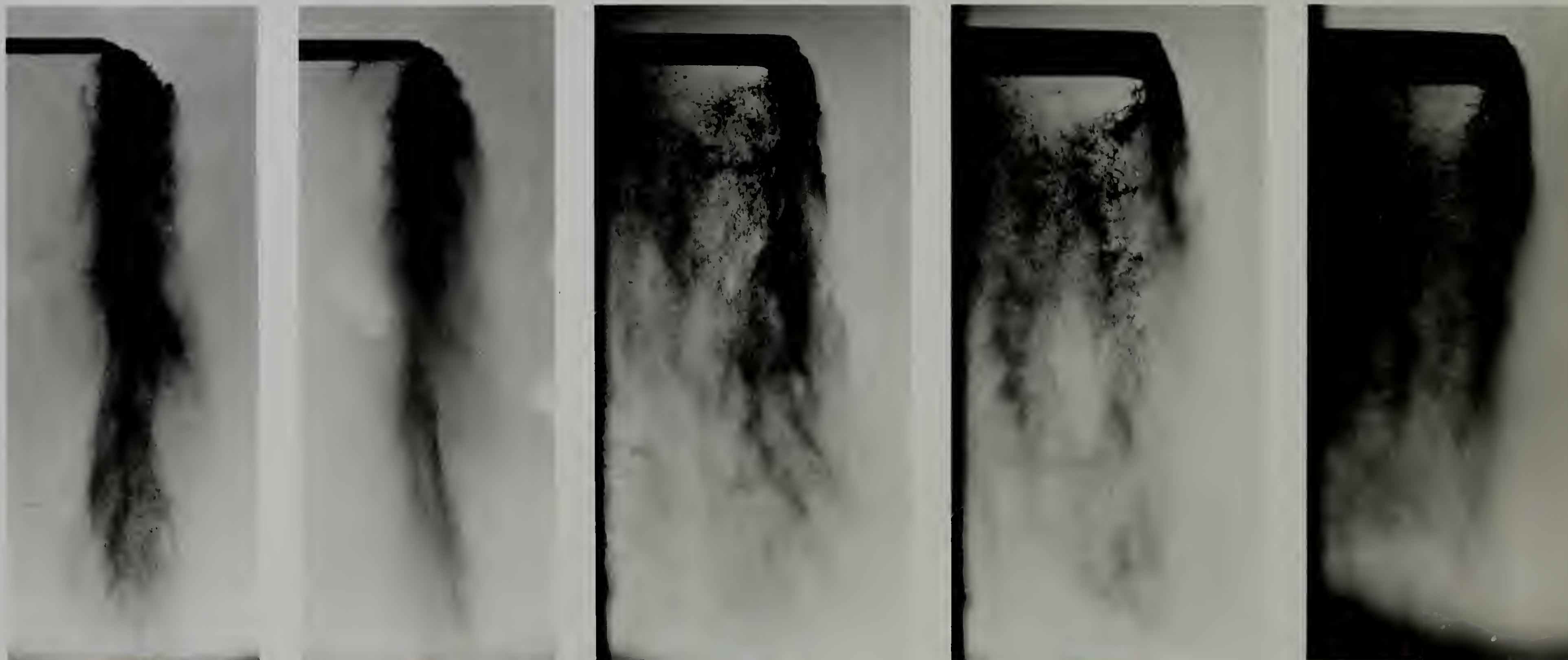

146 140 134 128 122

FIG. XXVII Fuel 3.34 gms./sec.
Air 660 ft./sec.

UPSTREAM INJECTION

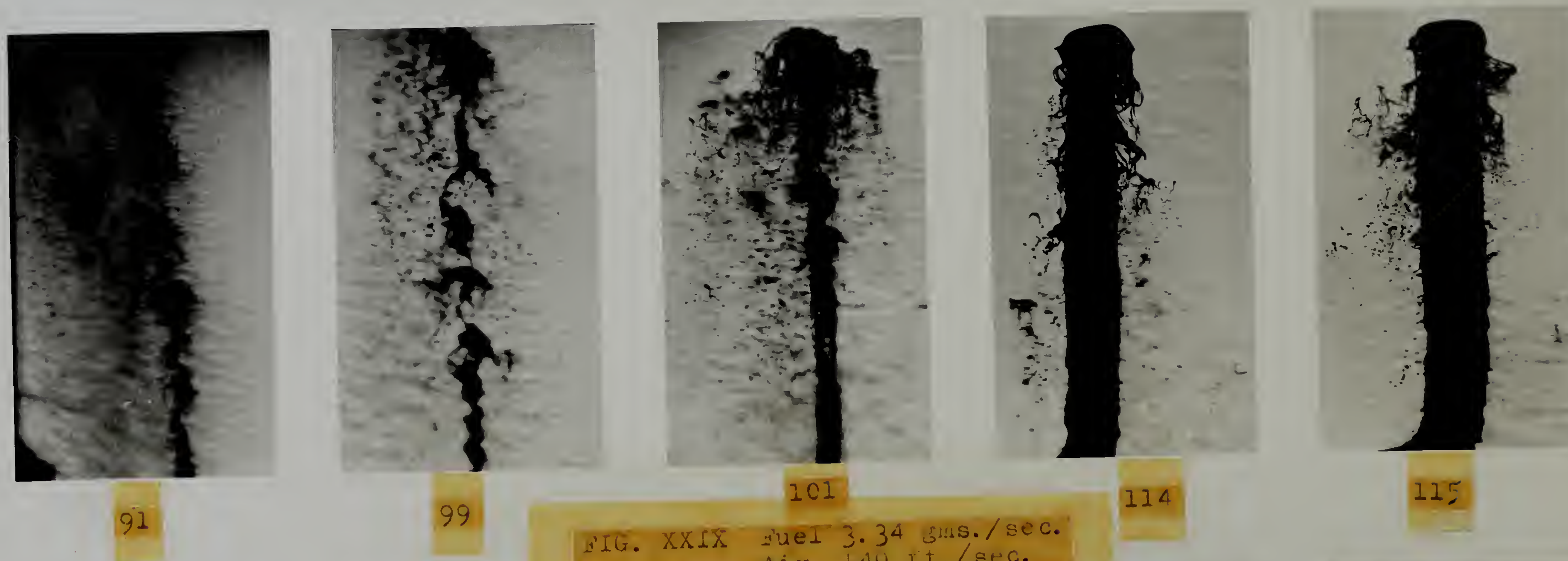

FIG. XXIX Fuel 3.34 gms./sec.
Air 140 ft./sec.

FIG. XXVIII Fuel 1.08 gms./sec.
Air 140 ft./sec.

87 97 106 112 118

FIG. XXXI Fuel 3.34 gms./sec.
Air 275 ft./sec.

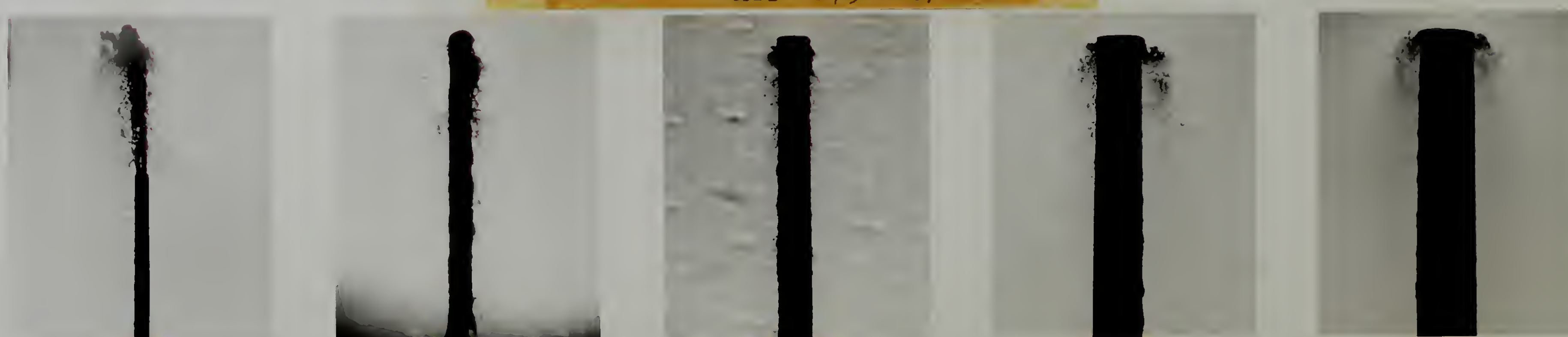

88 96 104 111 117

FIG. XXX Fuel 1.08 gms./sec.
Air 275 ft./sec.

FIG. XXXIII Fuel 3.34 gms./sec.
Air 660 ft./sec.

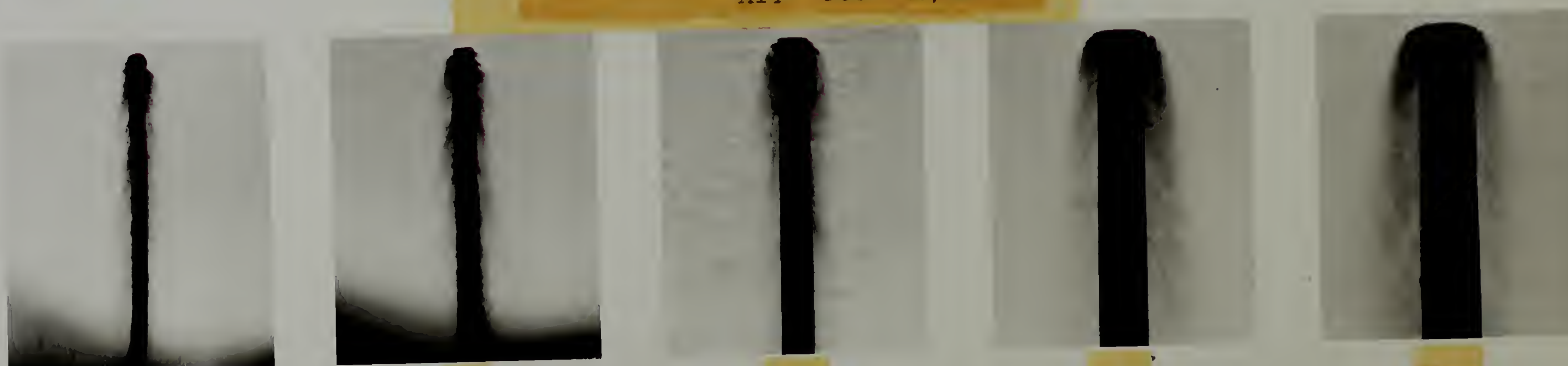

FIG. XXXII Fuel 1.08 gms./sec.
Air 660 ft./sec.

APPENDIX

APPENDIX A

SYMBOLS

Ac - Chamber area - in.^{2}

Ai - Nozzle area, inside - in.^{2}

d_f - Density of fuel - 0.83 gms./cm.^{3}

Di - Nozzle diameter, inside - in.

Do - Nozzle diameter, outside - in.

ΔPa - Differential air pressure - in. hg.

Pc - Chamber pressure - in. hg., gage.

Pca - Chamber pressure - psia.

Pd - Diffuser outlet pressure - in. hg., gage.

Pf - Fuel pump pressure - psi.

ΔPf - Differential fuel pressure - in. hg.

Po - Static pressure downstream of air nozzle - in. hg., gage.

Poa - Static pressure downstream of air nozzle - psia.

R - Gas constant for air - 53.34 ft. lb./lb. ^{o}Fabs.

Re - Reynolds' number.

t_a - Air temperature before diffuser - ^{o}F.

Ta - Air temperature before diffuser - ^{o}F abs.

Va - Air velocity in chamber - ft./sec.

Vf - Fuel velocity at nozzle tip - ft./sec.

Wa - Air weight rate - lb/min. or gms./sec., as indicated.

Wf - Fuel weight rate - gms./sec.

APPENDIX A

SYMBOLS

A_c - Chamber area - in.^{2}

A_i - Nozzle area, inside - in.^{2}

d_f - Density of fuel - 0.83 gms./cm.^{3}

D_i - Nozzle diameter, inside - in.

D_o - Nozzle diameter, outside - in.

ΔP_a - Differential air pressure - in. hg.

P_c - Chamber pressure - in. hg., gage.

P_{ca} - Chamber pressure - psia.

P_d - Diffuser outlet pressure - in. hg., gage.

P_f - Fuel pump pressure - psi.

ΔP_f - Differential fuel pressure - in. hg., gage.

P_o - Static pressure downstream of air nozzle - in. hg., gage.

P_{oa} - Static pressure downstream of air nozzle - psia.

R - Gas constant for air - 53.34 ft. lb./lb. ^{o}F abs.

R_e - Reynolds' number.

t_a - Air temperature before diffuser - ^{o}F.

T_a - Air temperature before diffuser - ^{o}F abs.

V_a - Air velocity in chamber - ft./sec.

V_f - Fuel velocity at nozzle tip - ft./sec.

W_a - Air weight rate - lb/min. or gms./sec., as indicated.

W_f - Fuel weight rate - gms./sec.

APPENDIX B

SUPPLEMENTARY INTRODUCTION

The atomization of liquids is important for many uses, such as spraying insecticides and paints, laying military smoke screens, and in drying and evaporation operations; but perhaps the most important use is in fuel burning power devices. In the latter it is essential that the fuel be finely atomized to permit intimate mixing of the fuel with as great a surface/volume ratio as possible, and that the fuel be mixed as rapidly as possible with the proper amount of air for combustion.

The characteristics most often used to describe a spray are:

1. Drop size - diameter of the individual particles in the spray.
2. Uniformity - deviation of the drop size from the mean.
3. Intensity - weight rate of flow of fluid per steradian.
4. Dispersion - Ratio of spray volume to liquid volume.
5. Distribution - Ratio of weight of air to fuel at any point in the spray.
6. Penetration - Farthest distance from the orifice along the axis of the spray reached by the spray.

APPENDIX B

SUPPLEMENTARY INTRODUCTION

The atomization of liquids is important for many uses, such as spraying insecticides and paints, laying military smoke screens, and in drying and evaporation operations; but perhaps the most important use is in fuel burning power devices. In the latter it is essential that the fuel be finely atomized to permit intimate mixing of the fuel with as great a surface/volume ratio as possible, and that the fuel be mixed as rapidly as possible with the proper amount of air for combustion.

The characteristics most often used to describe a spray are:

1. Drop size - diameter of the individual particles in the spray.
2. Uniformity - deviation of the drop size from the mean.
3. Intensity - weight rate of flow of fluid per steradian.
4. Dispersion - ratio of spray volume to liquid volume.
5. Distribution - ratio of weight of air to fuel at any point in the spray.
6. Penetration - farthest distance from the orifice along the axis of the spray reached by the spray.

7. Penetration rate - Velocity of the spray tip along its axis.
8. Cone angle - The total plane angle between the sides of the spray cone at its apex.

The physical variables affecting the spray characteristics are liquid nozzle geometry, spray container geometry, gas duct geometry, liquid characteristics and gas characteristics. Some theoretical considerations have been made to determine the effect of the above variables on the spray, but quantitative relations are lacking for want of sufficient generalized data.

The generally accepted theory of atomization is that proposed by Castleman (8), who assumes that atomization is the same for solid injection and air injection systems, depending only upon the relative velocity of the gas and liquid. His ligament theory is that droplets form as a consequence of small filaments of liquid being drawn out by the action of air on the main stream of the fuel jet. According to an earlier investigation by Rayleigh (10), the stability of a cylinder of liquid being drawn out and decreasing in diameter for any reason whatsoever decreases as the length of the cylinder is increased in comparison to the diameter of the cylinder. At the point where the length/diameter ratio becomes greater than the circumference of the cylinder, a decided instability is present and the action of surface tension is enough to cause the cylinder of liquid to collapse into droplets. At low air velocities drops are formed directly

7. Penetration rate - Velocity of the spray tip along its axis.
8. Cone angle - The total plane angle between the sides of the spray cone at its apex.

The physical variables affecting the spray characteristics are liquid nozzle geometry, spray container geometry, gas duct geometry, liquid characteristics and gas characteristics. Some theoretical considerations have been made to determine the effect of the above variables on the spray, but quantitative relations are lacking for want of sufficient generalized data.

The generally accepted theory of atomization is that proposed by Castleman (8), who assumes that atomization is the same for solid injection and air injection systems, depending only upon the relative velocity of the gas and liquid. His filament theory is that droplets form as a consequence of small filaments of liquid being drawn out by the action of air on the main stream of the fuel jet. According to an earlier investigation by Rayleigh (10), the stability of a cylinder of liquid being drawn out and decreasing in diameter for any reason whatsoever decreases as the length of the cylinder is increased in comparison to the diameter of the cylinder. At the point where the length/diameter ratio becomes greater than the circumference of the cylinder, a decided instability is present and the action of surface tension is enough to cause the cylinder of liquid to collapse into droplets. At low air velocities drops are formed directly from the jet by surface tension alone, at high velocities are formed by the combined action of ligament formation by the air and surface tension, while at high orifice Reynolds' numbers drop formation is further augmented by the turbulence of the liquid stream.

Haenlein (18) found that drop formation occurs by four separate mechanisms. At low relative velocity of liquid and air, the air does not appreciably affect the jet. Here the major factor in drop formation is the liquid surface tension, under the influence of which, rotationally symmetrical disturbances are set up in the column which increase until drops are formed. As air velocity increases, the amplitude of the disturbance increases, due to the high air velocity in the peaks and the low air velocity in the troughs of the liquid column. When the velocity is further increased, the initial disturbances become one-sided due to the augmented influence of the air on the column. The surface tension in this case retards wave formation since it tends to return the liquid column to its original form. At this point, the Castleman effect can be seen in liquids of low viscosity. Filaments are torn from the main stream and small drops are formed. With still further increase of velocity, filaments are formed closer and closer to the nozzle until all that can be seen is a cloud of droplets issuing directly from the orifice.

from the jet by surface tension alone, at high velocities are formed by the combined action of ligament formation by the air and surface tension, while at high orifice Reynolds' numbers drop formation is further augmented by the turbulence of the liquid stream.

Haenlein (13) found that drop formation occurs by four separate mechanisms. At low relative velocity of liquid and air, the air does not appreciably affect the jet. Here the major factor in drop formation is the liquid surface tension, under the influence of which, rotationally symmetrical disturbances are set up in the column which increase until drops are formed. As air velocity increases, the amplitude of the disturbance increases, due to the high air velocity in the peaks and the low air velocity in the troughs of the liquid column. When the velocity is further increased, the initial disturbances become one-sided due to the augmented influence of the air on the column. The surface tension in this case retards wave formation since it tends to return the liquid column to its original form. At this point, the Castleman effect can be seen in liquids of low viscosity. Filaments are torn from the main stream and small drops are formed. With still further increase of velocity, filaments are formed closer and closer to the nozzle until all that can be seen is a cloud of droplets issuing directly from the orifice.

The generally accepted theory of atomization, then, is that at low air velocities drops are formed directly from the jet by surface tension alone; at high air velocities drops are formed by the combined action of ligament formation by the air and of surface tension; while at high orifice Reynolds' numbers drop formation is further augmented by the turbulence of the liquid stream.

The generally accepted theory of atomization, then, is that at low air velocities drops are formed directly from the jet by surface tension alone; at high air velocities drops are formed by the combined action of ligament formation by the air and of surface tension; while at high orifice Reynolds' numbers drop formation is further augmented by the turbulence of the liquid stream.

APPENDIX C

EQUIPMENT DATA

Compressor:

"Ro-Twin" - Allis Chalmers Manufacturing Co., Milwaukee, Wisconsin.

Delivery - 533 cubic feet per minute at 100 psi gage.

Speed - 700 RPM

Compressor Motor:

General Electric Induction Type.

220 v., 60 cycle, 3 phase, 180 amp., 75 H.P.

860 RPM

Fuel Pump:

"Gerator" gear type.

Fuel Pump motor:

General Electric Split Phase Resistance

¼ H.P., 110 v., 60 cycle, 7.5 amp., 1725 RPM.

Camera:

"Voightlander" f 4.5, 9 x 12 cm. film pack.

Lens: Wirgin, f 3.5, 7.5 cm. focal length.

Film: Eastman "Plus-X".

Spark Power Pack:

Rectifier Transformer: Sola Gas Tube Transformer, 115 volt input, 15,000 volt output, 825 v.a., 60 ma.

Filament Transformer: "Thordarsen Multivolt" Electric Manufacturing Company, Chicago. Type 1-11F61, 63 watt.

Condenser: .01 mfd.

APPENDIX C

EQUIPMENT DATA

Compressor:

"Ro-Twin" - Allis Chalmers Manufacturing Co., Milwaukee, Wisconsin.

Delivery - 533 cubic feet per minute at 100 psi gage.

Speed - 700 RPM.

Compressor Motor:

General Electric Induction Type.

220 v., 60 cycle, 3 phase, 180 amp., 75 H.P.

860 RPM

Fuel Pump:

"Gerotor" gear type.

Fuel Pump Motor:

General Electric Split Phase Resistance

¼ H.P., 110 v., 60 cycle, 7.5 amp., 1725 RPM.

Camera:

"Voightlander" f 4.5, 9 x 12 cm. film pack.

Lens: "Heliar", f 3.5, 7.5 cm. focal length.

Film: Eastman "Plus-X".

Spark Power Pack:

Rectifier Transformer: Neon Gas Tube Transformer, 115 volt input, 15,000 volt output, 825 v.a., 60 ma.

Filament Transformer: "Thordarson Multivolt" Electric Manufacturing Company, Chicago. Type T-21F61, 63 watt.

Condenser: .01 mfd.

Rectifier Tube: Raytheon RKR-7Z.

Resistances: 5 megohm in each lead to condenser.

Spark Gap: ¼" stainless steel rods with ½" gap.

APPENDIX D

NOZZLE DATA

Each nozzle consists of a polished stainless steel tube tapered at the end and silver soldered to special brass adapters which screw into one of the metal walls, being held there by a nut and two lock washers, as shown in Figure IV. The other end of the adapters connects to a one-half inch brass fuel line. The nozzles were aligned in the adapters so that when the end of the adapter was flush with the metal wall, the nozzle tip was in the center of the chamber cross-section, and in the case of the bent nozzles, the bent portion was also aligned vertically, parallel to the chamber walls.

The nozzle tips were tapered to give a minimum interference between the air and fuel streams at the tip due to wall thickness. The taper was gradual, starting approximately one-half inch from the end, and the maximum taper of any one nozzle did not exceed 1½ degrees, thereby assuring almost uni-directional flow of air along the nozzle at the taper.

No attempt, other than polishing, was made to streamline that part of the nozzles which lay across the air stream. In the case of the five nozzles bent for upstream and downstream injection, that portion of the nozzle which lay along the air stream was made sufficiently long to allow the disturbed air, caused by the cross-stream part of the nozzle, to regain its uni-directional flow once again before reaching the tip.

APPENDIX D

NOZZLE DATA

Each nozzle consists of a polished stainless steel tube tapered at the end and silver soldered to special brass adapters which screw into one of the metal walls, being held there by a nut and two lock washers, as shown in Figure IV. The other end of the adapters connects to a one-half inch brass fuel line. The nozzles were aligned in the adapters so that when the end of the adapter was flush with the metal wall, the nozzle tip was in the center of the chamber cross-section, and in the case of the bent nozzles, the bent portion was also aligned vertically, parallel to the chamber walls.

The nozzle tips were tapered to give a minimum interference between the air and fuel streams at the tip due to wall thickness. The taper was gradual, starting approximately one-half inch from the end, and the maximum taper of any one nozzle did not exceed 1½ degrees, thereby assuring almost uni-directional flow of air along the nozzle at the taper.

No attempt, other than polishing, was made to streamline that part of the nozzles which lay across the air stream. In the case of the five nozzles bent for upstream and downstream injection, that portion of the nozzle which lay along the air stream was made sufficiently long to allow the disturbed air, caused by the cross-stream part of the nozzle, to regain its uni-directional flow once again before reaching the tip.

Each tip was measured on a metallograph at a magnification of 10.3 to 1. The outside diameters before the taper were measured with a micrometer.

Nozzle	Gage	Diameter Outside at Tip	Diameter Inside at Tip	Wall Thickness at Tip	Diameter Outside before taper
1 Bent	10	0.1080"	0.1050"	0.0015"	0.1330"
1 Perp.	10	0.1100	0.1020	0.0040	0.1280
2 Bent	12	0.0910	0.0845	0.0033	0.1070
2 Perp.	12	0.0950	0.0860	0.0045	0.1030
3 Bent	15	0.0610	0.0550	0.0030	0.0710
3 Perp.	15	0.0650	0.0550	0.0050	0.0710
4 Bent	18	0.0400	0.0340	0.0030	0.0470
4 Perp.	18	0.0380	0.0350	0.0015	0.0460
5 Bent	20	0.0320	0.0230	0.0045	0.0340
5 Perp.	20	0.0320	0.0230	0.0045	0.0340

PROPERTIES OF U. S. NAVY DIESEL OIL

Flash point, closed cup, min.	150 °F
Pour point	0 °F
Cloud point	10 °F
Viscosity, Saybolt Seconds Universal	40
Water and sediment, max.	trace
Total sulphur, max.	1.00%
Carbon residue, on 10% bottoms, max.	0.20%
Ash, max.	0.01%
Corrosion at 212°F, copper strips	Passable
90% distillation temperature, max.	675 °F
Color, max.	5
Ignition quality, min. Centane number	50
Density, gms./cm.^{3}	0.83
Surface tension, dynes/cm.	25.0

Each tip was measured on a metallograph at a magnification of 10.3 to 1. The outside diameters before the taper were measured with a micrometer.

Nozzle	Gage	Diameter Outside at Tip	Diameter Inside at Tip	Wall Thickness at Tip	Diameter Outside before taper
1 Bent	10	0.1080"	0.1050"	0.0015"	0.1330"
1 Perp.	10	0.1100	0.1020	0.0040	0.1280
2 Bent	12	0.0910	0.0845	0.0033	0.1070
2 Perp.	12	0.0950	0.0860	0.0045	0.1030
3 Bent	15	0.0610	0.0550	0.0030	0.0710
3 Perp.	15	0.0650	0.0550	0.0050	0.0710
4 Bent	18	0.0400	0.0340	0.0030	0.0470
4 Perp.	18	0.0380	0.0350	0.0015	0.0460
5 Bent	20	0.0320	0.0230	0.0045	0.0340
5 Perp.	20	0.0320	0.0230	0.0045	0.0340

PROPERTIES OF U. S. NAVY DIESEL OIL

Flash point, closed cup, min. . . . . 150 °F

Pour point . . . . 0 °F

Cloud point . . . . 10 °F

Viscosity, Saybolt Seconds Universal 40

Water and sediment, max. . . . . trace

Total sulphur, max. 1.00%

Carbon residue, on 10% bottoms, max. 0.20%

Ash, max. 0.01%

Corrosion at 212°F, copper strips . . . . . . Passable

90% distillation temperature, max. . . . . . . 675 °F

Color, max. 5

Ignition quality, min. Cetane number 50

Density, gms./cm.^{3} 0.83

Surface tension, dynes/cm. 25.0

APPENDIX E

CALIBRATION OF MANOMETERS

Fuel Manometer

The fuel mass rate was measured with a fuel over mercury manometer across a .025 sharp edged orifice in standard half-inch brass tubing. Differential pressure in inches of hg. across the orifice was plotted against fuel rate in grams per second. The data for this curve, Figure XXXIV, was obtained by weighing the fuel accumulated in a tared beaker in a given amount of time.

Measured Wt. Grams	Time of Run Seconds	Manometer In. of Hg.	Fuel Rate Gms./Sec.
93.90	181.1	.98	.518
179.22	170.2	3.84	1.052
140.68	90.4	7.74	1.557
137.00	68.4	11.87	2.002
163.20	71.0	15.75	2.30
186.25	71.2	20.11	2.620
181.00	63.0	24.21	2.870
177.85	54.7	30.52	3.245
184.50	52.0	35.67	3.545

Air Mass Rate

The air rate was measured by a standard one-inch sharp-edged orifice. Mass rate calibrations were made for this orifice for air by Dr. R. S. Bevans of the M.I.T. Staff, and Figure XXXV shows curves taken from his data. Differential pressure across the orifice was measured in inches of mercury with an air over mercury manometer. The static pressure down-

APPENDIX E

CALIBRATION OF MANOMETERS

Fuel Manometer

The fuel mass rate was measured with a fuel over mercury manometer across a .025 sharp edged orifice in standard half-inch brass tubing. Differential pressure in inches of hg. across the orifice was plotted against fuel rate in grams per second. The data for this curve, Figure XXXIV, was obtained by weighing the fuel accumulated in a tared beaker in a given amount of time.

Measured Wt. Grams	Time of Run Seconds	Manometer In. of Hg.	Fuel Rate Gms./Sec.
93.90	181.1	.96	.518
179.22	170.2	3.84	1.052
140.68	90.4	7.76	1.557
137.00	68.4	11.67	2.002
163.20	71.0	15.75	2.30
186.25	71.2	20.11	2.620
181.00	63.0	24.21	2.870
177.85	54.7	30.52	3.245
184.50	52.0	35.67	3.545

Air Mass Rate

The air rate was measured by a standard one-inch sharp-edged orifice. Mass rate calibrations were made for this orifice for air by Dr. E. S. Stevens of the M.I.T. Staff, and Figure XXXV shows curves taken from his data. Differential pressure across the orifice was measured in inches of mercury with an air over mercury manometer. The static pressure downstream from the orifice was measured with an open end mercury manometer in inches. The air temperature was measured at the entrance to the diffuser and the correction to the mass rate made as indicated on the figure.

Chamber Pressure

Because the chamber had to be removed frequently in order to change nozzles and clean the transparent walls, it was deemed impractical to install a permanent static pressure tap in the chamber for measuring chamber pressure. Instead, calibration curves (Figure XXXVI) were constructed between a permanent pressure tap in the 4" x 4" section at the outlet from the air diffuser and a temporary pressure tap replacing the fuel nozzle in the spray chamber. Two calibration curves were necessary for determining chamber pressure because the chamber exhaust piping was lengthened starting with Run 121, thereby influencing both the chamber pressure and the diffuser outlet pressure.

Original Chamber Exhaust Piping

Diffuser pressure (In.Hg.)	Chamber pressure (In.Hg.)
10.1	9.8
10.9	10.0
11.7	10.0
12.4	9.9
13.0	9.8
13.7	9.6
14.5	9.3
15.4	9.1
16.3	8.9
17.8	8.7
18.5	8.3
19.8	8.0
23.0	7.8

stream from the orifice was measured with an open end mercury manometer in inches. The air temperature was measured at the entrance to the diffuser and the correction to the mass rate made as indicated on the figure.

Chamber Pressure

Because the chamber had to be removed frequently in order to change nozzles and clean the transparent walls, it was deemed impractical to install a permanent static pressure tap in the chamber for measuring chamber pressure. Instead, calibration curves (Figure XLVI) were constructed between a permanent pressure tap in the 4" x 4" section at the outlet from the air diffuser and a temporary pressure tap replacing the fuel nozzle in the spray chamber. Two calibration curves were necessary for determining chamber pressure because the chamber exhaust piping was lengthened starting with Run 121, thereby influencing both the chamber pressure and the diffuser outlet pressure.

Original Chamber Exhaust Piping

Diffuser pressure (in.Hg.)	Chamber pressure (in.Hg.)
10.1	9.8
10.9	10.0
11.7	10.0
12.4	9.9
13.0	9.8
13.7	9.6
14.5	9.3
15.4	9.1
16.3	8.9
17.2	8.7
18.5	8.3
19.8	8.0
23.0	7.8

Modified Chamber Exhaust Piping

Diffuser pressure (In.Hg.)	Chamber pressure (In.Hg.)
7.4	7.0
8.1	7.2
9.0	7.3
9.8	7.3
10.5	7.3
11.3	7.2
12.3	7.1
13.0	6.9
14.2	6.6
15.4	6.4
16.8	6.1
19.4	5.8
22.8	5.9

Spark Timing

An attempt was made by Robillard to measure the duration of the spark and, consequently, the exposure time for the "instantaneous" photographs of the spray. He indicates that the exposure time is less than .25 x 10^{-7} seconds. No further attempt at physical measurement of the spark time was made by the authors, since it was felt that more accurate information than that given was not vital to a qualitative investigation.

Modified Chamber Exhaust Piping

Diffuser pressure (In.Hg.)	Chamber pressure (In.Hg.)
7.4	7.0
8.1	7.2
9.0	7.3
9.8	7.3
10.5	7.3
11.3	7.2
12.3	7.1
13.0	6.9
14.2	6.6
15.4	6.4
16.8	6.1
19.4	5.8
22.8	5.9

Spark Timing

An attempt was made by Robillard to measure the duration of the spark and, consequently, the exposure time for the "instantaneous" photographs of the spray. He indicates that the exposure time is less than 25 x 10^{-7} seconds. No further attempt at physical measurement of the spark time was made by the authors, since it was felt that more accurate information than that given was not vital to a qualitative investigation.

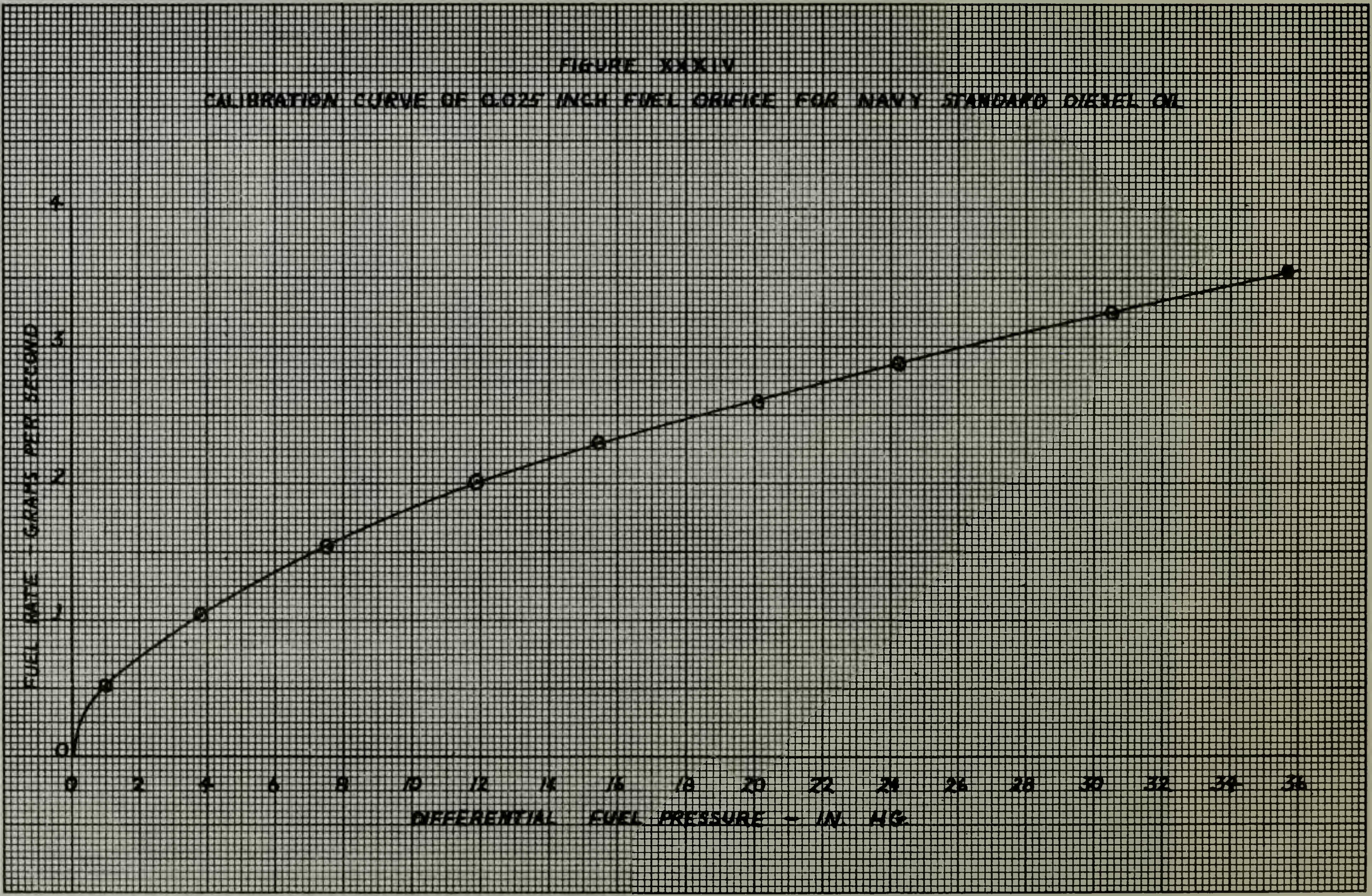

FIGURE XXXIV

CALIBRATION CURVE OF 0.025 INCH FUEL ORIFICE FOR NAVY STANDARD DIESEL OIL

FIGURE XXXV

CALIBRATION CURVE FOR ONE INCH AIR ORIFICE FROM DATA OF R. S. BEVANS
STATIC PRESSURE DOWNSTREAM OF ORIFICE - AIR TEMPERATURE 75F*

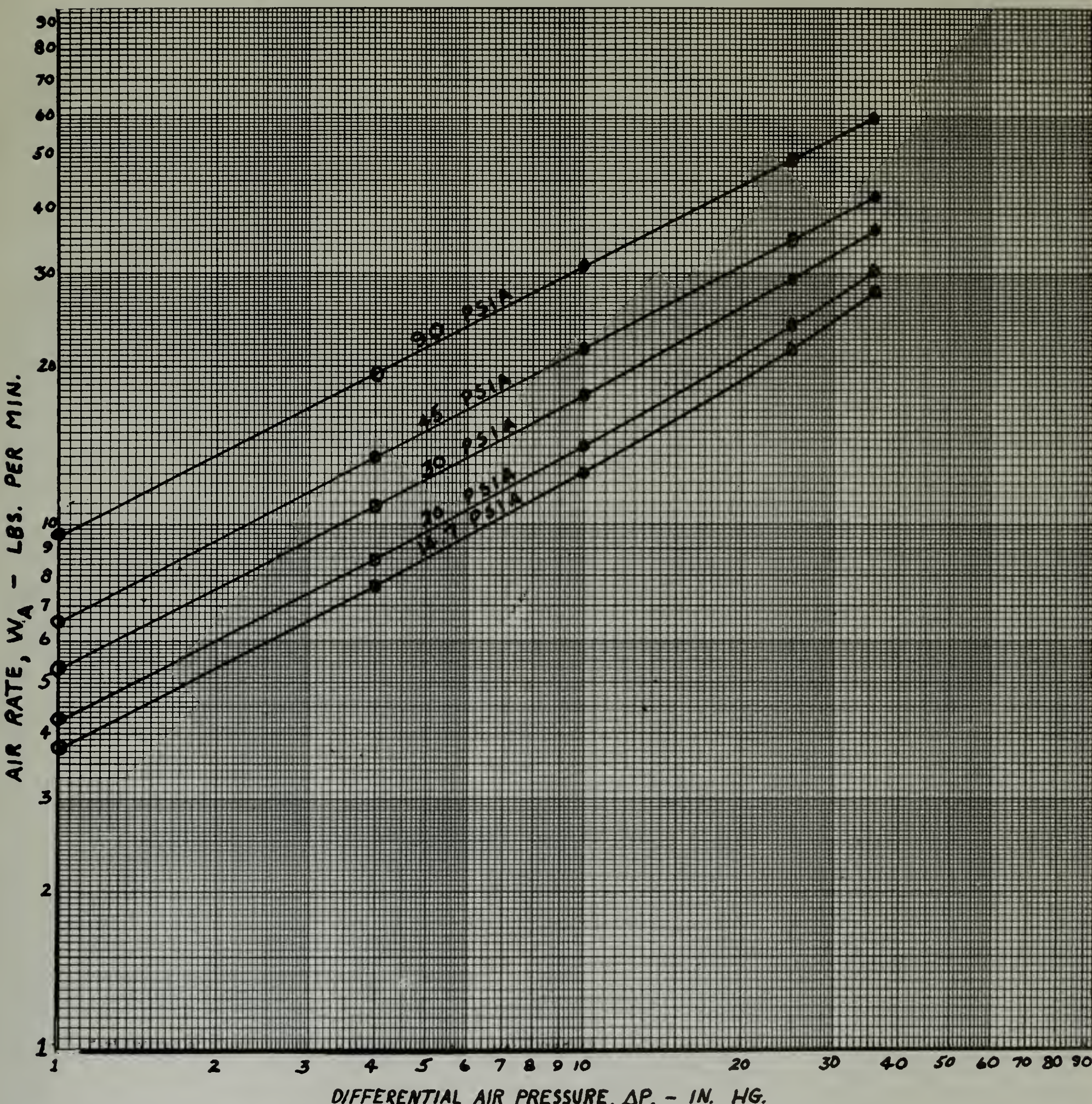

*AIR RATE CORRECTED FOR TEMPERATURE $= W_A(1.06 - 0.0008\, t°F)$

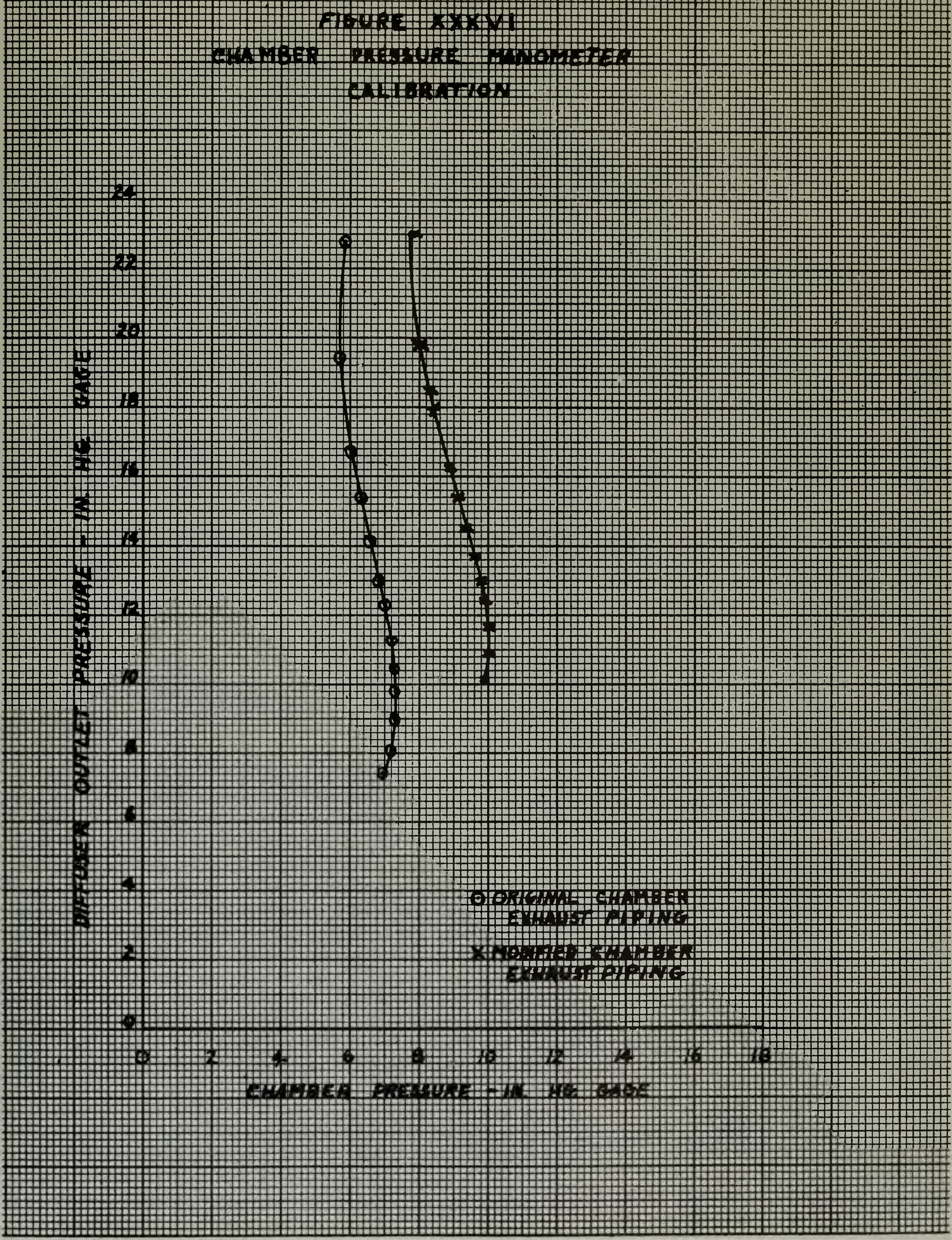
FIGURE XXXVI
CHAMBER PRESSURE MANOMETER
CALIBRATION
DIFFUSER OUTLET PRESSURE - IN. HG. GAGE
CHAMBER PRESSURE - IN. HG. GAGE
0 2 4 6 8 10 12 14 16 18
0 2 4 6 8 10 12 14 16 18 20 22 24
⊙ ORIGINAL CHAMBER EXHAUST PIPING
X MODIFIED CHAMBER EXHAUST PIPING

APPENDIX F

DATA AND CALCULATIONS

RUN	Δ Pa in.hg.	Δ Pf in.hg.	Po in.hg. gage	Pd in.hg. gage	Pc in.hg. gage	Poa psia	Pca psia	Wa gms./sec.	Wf gms./sec.	Va ft./sec.	Vf ft./sec.
17	25.0	32.6	14.2	16.1	6.2	21.7	17.7	180.5	3.37	665	49.5
25	25.5	32.2	14.6	16.4	6.1	21.9	17.7	182.5	3.35	673	8.7
26	6.0	32.2	7.0	8.9	7.3	18.1	18.3	78.0	3.35	278	8.7
29	1.7	32.1	6.6	7.8	7.1	17.9	18.2	40.4	3.34	145	8.6
34	26.0	4.0	12.8	16.7	6.1	21.0	17.7	183.0	1.08	675	2.8
39	6.2	33.2	8.2	9.0	7.3	18.7	18.3	79.5	3.40	284	22.8
40	25.1	32.2	11.9	16.1	6.2	20.5	17.7	179.0	3.35	660	22.5
50	25.0	31.1	14.1	16.1	6.2	21.6	17.7	179.0	3.27	660	3.5
51	6.2	30.8	8.8	9.0	7.3	19.0	18.3	80.1	3.26	286	3.5
53	1.7	3.8	7.4	7.8	7.1	18.3	18.2	41.0	1.05	147	1.1
54	1.7	31.0	8.0	7.8	7.1	18.6	18.2	41.0	3.27	147	3.5
74	25.0	32.0	14.2	16.1	6.2	21.7	17.7	181.5	3.34	669	2.4
75	5.9	32.0	8.9	8.9	7.3	19.1	18.3	78.0	3.34	278	2.4
77	1.8	3.8	7.5	7.8	7.1	18.4	18.2	41.8	1.05	150	0.7
79	1.6	4.0	7.1	7.4	7.0	18.2	18.1	38.8	1.10	140	16.2
80	1.6	32.0	7.0	7.4	7.0	18.1	18.1	38.8	3.34	140	49.0
85	27.4	3.3	13.7	17.5	6.0	21.4	17.6	191.1	.96	709	14.1
86	24.8	32.3	13.7	16.7	6.1	21.4	17.7	179.1	3.35	661	49.2
87	5.6	32.3	9.8	9.3	7.4	19.5	18.3	76.8	3.36	274	49.3
88	6.2	3.8	8.3	9.3	7.4	18.8	18.3	79.0	1.05	282	15.4
91	3.2	31.6	7.6	8.9	7.3	18.4	18.3	55.1	3.31	197	48.6
92	3.3	3.5	7.8	8.2	7.2	18.5	18.2	55.1	1.01	198	14.8
94	25.2	31.0	13.6	17.0	6.0	21.4	17.6	180.0	3.28	667	22.0
95	26.1	3.8	13.3	16.8	6.1	21.2	17.7	185.1	1.05	683	7.1
96	6.2	3.9	8.4	9.3	7.4	18.8	18.3	79.0	1.07	282	7.2
97	6.0	32.0	8.1	9.2	7.4	18.7	18.3	77.5	3.34	276	22.4
98	1.8	3.8	7.6	7.8	7.1	18.4	18.2	41.6	1.05	149	7.1
99	1.8	32.0	7.4	7.8	7.1	18.3	18.2	41.6	3.34	149	22.4
101	1.6	33.1	7.4	7.8	7.1	18.5	18.2	38.8	3.40	139	8.8
104	6.8	4.0	8.2	9.4	7.4	18.7	18.3	82.8	1.08	295	2.8

Run	Δ Pe in.hg.	Δ Pf in.hg.	Po in.hg. gage	Pd in.hg. gage	Pe in.hg. gage	Pon psia	Poe psia	Wa gms. sec.	Wf gms. sec.	Va ft. sec.	Vf ft. sec.
17	25.0	32.6	14.2	16.1	6.2	21.7	17.7	180.5	3.37	665	49.5
25	25.5	32.2	14.6	16.4	6.1	21.9	17.7	182.5	3.35	673	8.7
26	6.0	32.2	7.0	8.9	7.3	18.1	18.3	78.0	3.35	278	8.7
29	1.7	32.1	6.6	7.8	7.1	17.9	18.2	40.4	3.34	145	8.6
34	26.0	4.0	12.8	16.7	6.1	21.0	17.7	183.0	1.08	675	2.8
39	6.2	33.2	8.2	9.0	7.3	18.7	18.3	79.5	3.40	284	22.8
40	25.1	32.2	11.9	16.1	6.2	20.5	17.7	179.0	3.35	664	22.5
50	25.0	31.1	14.1	16.1	6.2	21.0	17.7	179.0	3.27	660	3.5
51	6.2	30.8	8.8	9.0	7.3	19.0	18.3	80.1	3.26	286	3.5
53	1.7	3.8	7.4	7.8	7.1	18.3	18.2	41.0	1.05	147	1.1
54	1.7	31.0	8.0	7.8	7.1	18.6	18.2	41.0	3.27	147	3.5
74	25.0	32.0	14.2	16.1	6.2	21.7	17.7	181.5	3.34	669	2.4
75	5.9	32.0	8.9	8.9	7.3	19.1	18.3	78.0	3.34	278	2.4
77	1.8	3.8	7.5	7.8	7.1	18.4	18.2	41.8	1.05	150	0.7
79	1.6	4.0	7.1	7.4	7.0	18.2	18.1	38.8	1.10	140	16.2
80	1.6	32.0	7.0	7.4	7.0	18.1	18.1	38.8	3.34	140	49.0
85	27.4	3.3	13.7	17.5	6.0	21.4	17.6	191.1	.96	709	14.1
86	24.8	32.3	13.7	16.7	6.1	21.4	17.7	179.1	3.33	661	49.2
87	5.6	32.3	9.8	9.3	7.4	19.5	18.3	76.8	3.36	274	49.3
88	6.2	3.6	8.3	9.3	7.4	18.8	18.3	79.0	1.05	282	15.4
91	3.2	31.6	7.6	8.9	7.3	18.4	18.3	55.1	3.31	197	48.6
92	3.3	3.5	7.8	8.8	7.2	18.5	18.2	55.1	1.01	198	14.8
94	25.2	31.0	13.6	17.0	6.0	21.4	17.6	180.0	3.28	667	22.0
95	26.1	3.8	13.3	16.8	6.1	22.2	17.7	185.1	1.05	683	7.1
96	6.2	3.9	8.4	9.3	7.4	18.8	18.3	79.0	1.07	282	7.2
97	6.0	32.0	8.1	9.2	7.4	18.7	18.3	77.5	3.34	276	22.4
98	1.8	3.8	7.6	7.8	7.1	18.4	18.2	41.6	1.05	149	7.1
99	1.8	32.0	7.4	7.8	7.1	18.3	18.2	41.6	3.34	149	22.4
101	1.6	33.1	7.4	7.8	7.1	18.5	18.2	38.8	3.40	139	8.8
104	6.8	4.0	8.8	9.4	7.4	18.7	18.3	82.8	1.08	295	2.8

RUN	Δ Pa in.hg.	Δ Pf in.hg.	Po in.hg. gage	Pd in.hg. gage	Pc in.hg. gage	Poe psia	Poa psia	Wa gms./sec.	Wf gms./sec.	Va ft./sec.	Vf ft./sec.
105	2.4	4.0	7.6	8.0	7.2	18.8	18.2	47.6	1.08	171	2.8
106	6.0	32.6	8.9	10.0	7.4	19.1	18.3	78.2	3.37	279	8.7
107	24.9	30.2	17.2	20.0	5.7	23.2	17.5	185.1	3.23	691	8.3
108	24.5	3.8	14.6	16.7	6.1	21.9	17.7	178.2	1.05	656	2.7
109	24.5	3.6	13.1	16.5	6.1	21.1	17.7	178.2	1.01	656	1.1
110	25.4	32.6	13.7	17.1	6.0	21.4	17.6	183.0	3.36	679	3.6
111	5.9	4.0	8.9	9.3	7.4	19.1	18.3	80.0	1.08	266	1.2
112	6.2	33.4	8.2	9.3	7.4	18.7	18.3	78.2	3.41	279	3.7
113	1.8	3.9	7.7	7.8	7.1	18.5	18.2	41.6	1.07	149	1.2
114	1.8	33.5	7.7	7.8	7.1	18.5	18.2	41.6	3.42	149	3.7
115	1.8	31.7	7.3	7.4	7.0	18.3	18.1	41.6	3.31	150	2.3
116	1.7	3.6	7.2	7.6	7.1	18.2	18.2	40.2	1.01	145	0.7
117	6.1	3.9	8.0	9.0	7.3	18.6	18.3	77.5	1.07	276	0.8
118	6.1	31.3	8.0	9.1	7.4	18.6	18.3	77.5	3.30	276	2.3
119	25.6	4.0	13.9	17.6	6.0	21.5	17.6	184.6	1.08	685	0.8
120	25.5	31.8	13.9	17.6	6.0	21.5	17.6	184.6	3.32	685	2.4
				MODIFIED CHAMBER EXHAUST PIPING							
121	25.4	3.8	16.6	20.0	8.0	22.9	18.6	186.1	1.05	653	0.8
122	26.0	31.6	16.0	19.7	8.0	22.6	18.6	186.1	3.31	653	2.5
123	6.2	3.9	11.7	12.7	9.9	20.9	19.6	83.0	1.06	276	0.8
124	6.2	31.7	12.4	12.6	9.9	20.8	19.6	83.0	3.37	276	2.5
125	1.7	3.9	11.0	11.3	10.0	20.1	19.6	41.7	1.06	139	0.8
126	1.7	32.3	10.7	11.1	10.0	19.9	19.6	41.7	3.36	139	2.5
127	25.6	3.8	15.4	19.0	8.2	22.3	18.7	183.1	1.05	640	1.1
128	25.4	31.9	15.4	19.6	8.0	22.3	18.6	183.1	3.33	643	3.5
129	5.8	3.8	11.5	12.1	10.0	20.4	19.6	80.0	1.05	266	1.1
130	6.0	32.1	11.7	12.7	9.9	20.5	19.6	81.4	3.35	271	3.5
131	1.6	3.9	10.2	10.4	9.9	19.7	19.6	40.4	1.06	134	1.1
132	1.5	32.4	10.1	10.3	9.9	19.7	19.6	38.8	3.36	129	3.5
133	24.0	3.8	15.1	18.4	8.3	22.1	18.8	179.0	1.05	621	2.8
134	26.0	32.7	15.7	19.2	8.1	22.4	18.7	185.8	3.38	648	9.0

RUN	Δ Pa in.hg.	Δ Pf in.hg.	Po in.hg. gage	Pd in.hg. gage	Pc in.hg. gage	Poa psia	Pca psia	Wa gms./sec.	Wf gms./sec.	Va ft./sec.	Vf ft./sec.
135	6.2	4.1	11.5	12.5	9.9	20.4	19.6	82.1	1.09	274	2.9
136	6.2	32.5	11.4	12.2	10.0	20.3	19.6	82.1	3.37	274	9.0
137	1.7	3.7	10.5	10.9	10.0	20.4	19.6	42.0	1.03	140	2.7
138	1.7	32.6	11.3	10.8	10.0	20.3	19.6	42.0	3.33	140	8.9
140	25.6	32.3	15.8	19.1	8.1	22.5	18.7	184.0	3.36	642	21.3
141	5.6	3.7	12.0	13.3	9.7	20.6	19.5	79.2	1.03	266	6.5
142	6.2	32.5	12.2	12.7	9.9	20.7	19.6	82.9	3.37	276	21.4
143	1.7	4.1	10.9	11.2	10.0	20.1	19.6	41.7	1.09	139	6.9
144	1.7	18.4	10.7	10.8	10.0	19.9	19.6	41.1	2.50	137	15.9
145	25.7	4.0	15.7	19.2	8.1	22.4	18.7	184.0	1.08	642	15.9
146	25.5	32.5	16.8	20.4	7.9	23.0	18.6	186.1	3.37	653	49.5
148	5.8	3.9	12.5	12.7	9.9	20.8	19.6	80.6	1.06	268	15.6
149	6.2	27.0	11.3	12.7	9.9	20.3	19.6	82.0	3.05	274	44.8
150	1.7	4.3	11.0	11.2	10.0	20.1	19.6	41.7	1.12	139	16.5
151	1.7	32.5	10.6	11.2	10.0	19.9	19.6	41.1	3.37	137	49.5
152	6.0	4.1	11.2	12.3	10.0	20.2	19.6	81.4	1.09	271	1.2
153	6.1	3.8	11.2	12.3	10.0	20.2	19.6	81.4	1.05	271	1.1
154	6.1	3.8	11.2	12.3	10.0	20.2	19.6	81.4	1.05	271	1.1
155	26.0	4.2	16.5	19.9	8.0	22.8	18.6	188.8	1.10	661	1.2
157	25.9	4.2	16.8	20.4	7.9	23.0	18.6	187.9	1.10	659	0.8
158	5.6	4.1	11.8	12.4	10.0	20.5	19.6	78.5	1.09	262	0.8
159	6.0	4.1	11.0	12.0	10.0	20.1	19.6	81.4	1.09	271	0.8
160	6.0	4.0	11.0	12.0	10.0	20.1	19.6	81.4	1.08	271	0.8
161	1.6	31.0	10.3	10.3	9.9	19.7	19.6	40.4	3.28	135	2.3
165	6.6	3.8	11.3	12.3	10.0	20.3	19.6	83.6	1.05	278	0.7
167	6.2	3.9	10.6	11.7	10.0	19.9	19.6	81.4	1.06	271	2.7
168	6.2	4.2	10.7	11.7	10.0	19.9	19.6	81.4	1.10	271	2.8
169	6.2	4.1	10.7	11.7	10.0	19.9	19.6	81.4	1.09	271	2.8
170	1.6	4.1	10.2	10.5	10.0	19.7	19.6	40.4	1.09	135	2.8
171	6.1	4.0	10.7	11.7	10.0	19.9	19.6	79.2	1.08	264	7.3

RUN	ΔPa in.hg.	ΔPf in.hg.	Po in.hg. gage	Pd in.hg. gage	Pc in.hg. gage	Poa psia	Pca psia	Wa gms./sec.	Wf gms./sec.	Va ft./sec.	Vf ft./sec.
172	6.1	4.1	10.7	11.7	10.0	19.9	19.6	79.9	1.09	266	7.3
173	6.1	4.1	10.7	11.7	10.0	19.9	19.6	79.9	1.09	266	7.3
174	26.0	4.1	17.0	20.1	8.0	23.1	18.6	189.8	1.09	665	7.3
175	1.8	4.2	11.1	11.3	10.0	20.2	19.6	43.1	1.10	144	7.4
177	1.7	33.2	10.3	10.7	10.0	19.8	19.6	41.0	3.41	137	22.9
178	6.2	4.1	11.0	11.5	10.0	20.1	19.6	81.9	1.09	272	16.0
179	6.2	4.0	11.0	11.5	10.0	20.1	19.6	81.9	1.08	272	15.9
180	6.2	4.0	11.0	11.5	10.0	20.1	19.6	81.9	1.08	272	15.9
181	6.2	32.1	11.0	11.5	10.0	20.1	19.6	81.9	3.35	272	49.2
182	25.7	3.9	16.4	19.7	8.0	22.8	18.6	186.0	1.07	653	15.7
184	5.9	4.0	11.0	12.3	10.0	20.1	19.6	80.5	1.08	268	15.9
185	6.0	32.2	11.1	12.4	9.9	20.2	19.6	81.2	3.36	270	49.4
186	24.8	32.1	15.1	19.3	8.1	22.1	18.7	178.8	3.35	624	49.2
188	25.0	4.0	15.7	20.1	8.0	22.4	18.6	182.1	1.08	640	15.9
190	1.5	4.0	10.1	10.3	9.9	19.7	19.6	38.7	1.08	129	15.9
191	1.5	32.1	10.1	10.3	9.9	19.7	19.6	38.7	3.35	129	49.2
192	6.2	4.1	11.3	12.7	9.9	20.3	19.6	82.0	1.09	273	7.3
193	6.1	32.2	11.2	12.3	10.0	20.2	19.6	82.0	3.36	273	22.6
194	25.0	4.0	15.7	20.2	8.0	22.4	18.6	182.1	1.08	640	7.3
195	24.8	31.8	15.1	19.3	8.1	22.1	18.7	178.8	3.33	624	22.4
197	1.7	4.1	11.0	11.3	10.0	20.1	19.6	41.6	1.09	139	7.3
198	1.7	31.8	11.0	11.3	10.0	20.1	19.6	41.6	3.33	139	22.4
199	25.2	4.1	13.6	17.0	8.7	21.4	19.0	180.0	1.09	618	2.8
200	24.9	32.0	13.5	16.7	8.8	20.4	19.0	177.8	3.34	610	8.6
201	6.3	4.0	10.7	11.8	10.0	20.0	19.6	82.0	1.08	272	2.8
202	6.2	32.0	11.3	12.7	9.9	20.3	19.6	82.0	3.34	272	8.6
203	1.7	3.8	10.5	10.9	10.0	19.9	19.6	41.6	1.05	139	2.7
204	1.7	31.6	10.5	10.9	10.0	19.9	19.6	41.6	3.32	139	8.6
206	1.5	32.0	10.1	10.5	9.9	19.7	19.6	38.7	3.34	129	3.6
207	6.2	4.2	12.2	12.7	9.9	20.7	19.6	82.0	1.10	273	1.2

RUN	ΔPa in.hg.	ΔPf in.hg.	Po in.hg. gage	Pd in.hg. gage	Pc in.hg. gage	Poa psia	Pca psia	Wa gms./sec.	Wf gms./sec.	Va ft./sec.	Vf ft./sec.
208	6.0	31.8	11.7	12.7	9.9	20.5	19.6	80.5	3.33	268	3.6
209	25.7	32.3	15.8	19.2	8.1	22.5	18.7	186.0	3.36	650	3.6
210	24.6	4.0	13.1	16.6	8.8	21.2	19.0	178.8	1.08	614	1.2
211	1.6	4.1	10.3	10.4	9.9	19.8	19.6	39.4	1.09	131	0.8
212	1.5	32.1	10.1	10.3	9.9	19.7	19.6	38.7	3.35	129	2.4
214	5.8	32.2	12.5	12.7	9.9	20.9	19.6	80.5	3.36	268	2.4
215	24.8	4.0	15.1	19.3	8.1	22.1	18.7	178.8	1.08	624	0.8
216	25.0	32.1	15.7	20.2	8.0	22.4	18.6	182.1	3.35	640	2.4
220	25.3	4.0	15.6	19.1	8.1	22.4	18.7	186.0	1.08	650	6.9
228	1.7	4.1	10.5	10.9	10.0	19.9	19.6	41.6	1.09	139	1.2

APPENDIX G

SAMPLE CALCULATIONS

Run 180 - Nozzle 5 Downstream with modified chamber exhaust piping.

Calculate: (1) Fuel weight rate, (2) fuel velocity, (3) air weight rate, and (4) air velocity.

Assume: (1) Compressible, steady state air flow in the constant area chamber. This assumption is valid for the maximum Mach number encountered, approximately 0.6.

(2) The temperature of the air preceding the air diffuser constant and equal to the temperature of the air in the chamber. The variation in temperature preceding the diffuser in all runs was no greater than four degrees and the maximum temperature difference between it and the chamber temperature was $10^{\circ}F$, this maximum occurring only at the highest air rate. To simplify tedious calculations, a mean temperature of $95^{\circ}F$ was used for all runs. The maximum error in air weight rate by this assumption was 2% at the highest air rate, less for lower air rates. Since the use of Figure XXXV gave an error of approximately 5%, this assumption was justified.

APPENDIX C

SAMPLE CALCULATIONS

Run 180 - Nozzle 5 Downstream with modified chamber exhaust piping.

Calculate: (1) Fuel weight rate, (2) fuel velocity, (3) air weight rate, and (4) air velocity.

Assume: (1) Compressible, steady state air flow in the constant area chamber. This assumption is valid for the maximum Mach number encountered, approximately 0.6.

(2) The temperature of the air preceding the air diffuser constant and equal to the temperature of the air in the chamber. The variation in temperature preceding the diffuser in all runs was no greater than four degrees and the maximum temperature difference between it and the chamber temperature was 10°F, this maximum occurring only at the highest air rate. To simplify tedious calculations, a mean temperature of 95°F was used for all runs. The maximum error in air weight rate by this assumption was 2% at the highest air rate, less for lower air rates. Since the use of Figure XXXV gave an error of approximately 5%, this assumption was justified.

SAMPLE CALCULATIONS
(Cont'd)

Given: $t_a = 95F$ $\quad T_a = 555F$ abs.

$Pf = 90$ psi.

$\Delta Pf = 4.0$ in. hg.

$\Delta Pa = 6.2$ in. hg.

$Pd = 11.5$ in. hg. gage

$Po = 11.0$ in. hg. gage $\quad Poa = 20.1$ psia.

$d_f = 0.83$ gms./cm.^{3}

$Di = 0.023$ in. $\quad Ai = 4.155 \times 10^{-4}$ in.^{2} for nozzle 5 Downstream

$Ac = 1.0$ in.^{2}

Solution: (1) With $\Delta Pf = 4.0$, enter curve, Figure XXXIV, read $Wf = 1.08$ gms./sec.

(2) $$Vf = \frac{W_f}{Ai\ d_f}$$

$$= \frac{1.08 \text{ gms./sec.}}{4.155 \times 10^{-4} \text{ in}^2 \ \ 0.83 \frac{\text{gms}}{\text{cm}^3} \ \ 6.45 \frac{\text{cm}^2}{\text{in}^2} \ \ 30.48 \frac{\text{cm.}}{\text{ft.}}}$$

$$= 15.9 \text{ ft./sec.}$$

(3) With $\Delta Pa = 6.2$ and $Poa = 20.1$ psia, enter curve, Figure XXXV, read $Wa = 11.0$ lb./min.

Wa (corrected for temperature)

$$= Wa\ (1.06 - 0.0008\ t_aF)$$

$$= 11.0\ (1.06 - 0.008 \times 95)$$

$$= 10.81 \text{ lb./min.}$$

$$= \frac{10.81 \text{ lb./min} \ \ 453.6 \text{ gms./lb.}}{60 \text{ sec./min.}}$$

$$= 81.9 \text{ gms./sec.}$$

Sample Calculations
(Cont'd)

Given: t_a = 95F Ta = 555F abs.

Pf = 90 psi.

ΔPf = 4.0 in. hg.

ΔPa = 6.2 in. hg.

Pd = 11.5 in. hg. gage

Po = 11.0 in. hg. gage Pom = 20.1 psia.

d_f = 0.83 gms./cm.^{3}

Dt = 0.023 in. At = 4.155 x 10^{-4} in.^{2} for nozzle 5 Downstream

Ao = 1.0 in.^{2}

Solution: (1) With ΔPf = 4.0, enter curve, Figure XXXIV, read Wf = 1.08 gms./sec.

(2) $Vf = \dfrac{W_f}{At\ d_f}$

$$= \frac{1.08 \text{ gms./sec.}}{4.155 \times 10^{-4} \text{ in.}^2 \ \ 0.83 \frac{\text{gms}}{\text{cm}^3} \ \ 6.45 \frac{\text{cm.}^2}{\text{in.}^2} \ \ 30.48 \frac{\text{cm.}}{\text{ft.}}}$$

= 15.9 ft./sec.

(3) With ΔPa = 6.2 and Pom = 20.1 psia, enter curve, Figure XXXV, read Wa = 11.0 lb./min.

Wa (corrected for temperature)

= Wa (1.06 - 0.0008 t_aF)

= 11.0 (1.06 - 0.008 x 95)

= 10.81 lb./min.

$$= \frac{10.81 \text{ lb./min } 453.6 \text{ gms./lb.}}{60 \text{ sec./min.}}$$

= 81.9 gms./sec.

SAMPLE CALCULATIONS
(Cont'd)

(4) With Pd = 11.5, enter curve, Figure XXXVI, modified chamber exhaust piping, read

Pc = 10.0 in. hg. gage, Pca = 19.6 psia.

Then $V_a = \frac{W_a \; R \; T_a}{P_{ca} \; A_c}$ where R is the gas constant for air = 53.34 ft. lb./lb. F abs.

$$= \frac{81.9 \frac{\text{gms.}}{\text{sec.}} \quad 53.34 \frac{\text{ft.lb.}}{\text{lb.F abs.}} \quad 555 \text{ F abs.}}{19.6 \frac{\text{lb.}}{\text{in.}^2} \quad 1.0 \text{ in.}^2 \quad 453.6 \frac{\text{gms.}}{\text{lb.}}}$$

= 272 ft./sec.

SAMPLE CALCULATIONS
(Cont'd)

(4) With Pd = 11.5, enter curve, Figure XXXVI, modified chamber exhaust piping, read

Pc = 10.0 in. Hg. gage, Pca = 19.6 psia.

Then $Va = \frac{Wa\ R\ Tc}{Pca\ \ Ac}$ where R is the gas constant for air = 53.34 ft. lb./lb. F abs.

$$= \frac{81.9\ \frac{gms.}{sec.}\ \ 53.34\ \frac{ft.lb.}{lb.F\ abs.}\ \ 555\ F\ abs.}{19.6\ \frac{lb.}{in.^2}\ \ 1.0\ in.^2\ \ 453.6\ \frac{gms.}{lb.}}$$

= 272 ft./sec.

APPENDIX H

LITERATURE CITATIONS

1. Sauter, J., "Determining Size of Drops in Fuel Mixture of Internal Combustion Engines", NACA T.R. 390, 1926.

2. Sauter, J., "Investigation of Atomization in Carburetors", NACA T.M. 518, 1929.

3. Lee, D. W., "The Effects of Nozzle Design and Operating Conditions on the Atomization and Distribution of Fuel Sprays", NACA T.R. 424, 1932.

4. Lee, D. W., "Photomicrographic Studies of Fuel Sprays", NACA T.R. 454, 1933.

5. Lee, D. W., "A Comparison of Fuel Sprays from Several Types of Injection Nozzles", NACA T.R. 520, 1935.

6. De Juhasz, K. J., "Results of Recent Oil Spray Research", Trans. ASME OGP-51-9, 1929.

7. De Juhasz, Zahn & Schweitzer, "On the Formation and Dispersion of Oil Sprays", Bulletin 40, Penn. State College Eng. Experimental Station, 1932.

8. Castleman, R. A., Jr., "The Mechanism of the Atomization of Liquids", Research Paper 281, Bar Standard Journal Research, March 1931.

9. Castleman, R. A., Jr., "Mechanism of Atomization Accompanying Solid Injections", NACA T.R. 440, 1932.

10. Rayleigh, Lord, "On the Instability of Jets", Proc. London Math. Soc., Vol. X, pp 4-13, 1878.

11. Longwell, J. P., "Fuel Oil Atomization", Sc.D. Thesis, M.I.T., Course X, 1941.

12. Kolupaev, P. G., "Atomization of Heavy Fuel Oil", Sc.D. Thesis, M.I.T. Course X, 1941.

13. Snuggs, J. F., "Atomization of Heavy Fuel Oils", S.M. Thesis, M.I.T. Course X, 1938.

14. Robillard, G., "Atomization of Liquid Fuels in an Airstream", S.M. Thesis, M.I.T., Course X, 1947.

APPENDIX H

LITERATURE CITATIONS

1. Sauter, J., "Determining Size of Drops in Fuel Mixture of Internal Combustion Engines", NACA T.R. 390, 1926.

2. Sauter, J., "Investigation of Atomization in Carburetors", NACA T.M. 518, 1929.

3. Lee, D. W., "The Effects of Nozzle Design and Operating Conditions on the Atomization and Distribution of Fuel Sprays", NACA T.R. 424, 1932.

4. Lee, D. W., "Photomicrographic Studies of Fuel Sprays", NACA T.R. 454, 1933.

5. Lee, D. W., "A Comparison of Fuel Sprays from Several Types of Injection Nozzles", NACA T.R. 520, 1935.

6. De Juhasz, K. J., "Results of Recent Oil Spray Research", Trans. ASME OGP-51-9, 1929.

7. De Juhasz, Zahn & Schweitzer, "On the Formation and Dispersion of Oil Sprays", Bulletin 40, Penn. State College Eng. Experimental Station, 1932.

8. Castleman, R. A., Jr., "The Mechanism of the Atomization of Liquids", Research Paper 281, Bur Standard Journal Research, March 1931.

9. Castleman, R. A., Jr., "Mechanism of Atomization Accompanying Solid Injections", NACA T.N. 440, 1932.

10. Rayleigh, Lord, "On the Instability of Jets", Proc. London Math. Soc., Vol. X, pp 4-13, 1878.

11. Longwell, J. P., "Fuel Oil Atomization", Sc.D. Thesis, M.I.T., Course X, 1941.

12. Kolupaev, P. G., "Atomization of Heavy Fuel Oil", Sc.D. Thesis, M.I.T. Course X, 1941.

13. Snuggs, J. F., "Atomization of Heavy Fuel Oils", S.M. Thesis, M.I.T. Course X, 1938.

14. Robillard, G., "Atomization of Liquid Fuels in an Airstream", S.M. Thesis, M.I.T., Course X, 1947.

LITERATURE CITATIONS
(Cont'd)

15. Nukiyama & Tanisawa, "An Experiment on the Atomization of Liquid", Report 1-6, Trans. Soc. Mech. Eng., Japan, 1938-1940.

16. British Fuel Research Board Report for the year ending March 31, 1938.

17. Lewis, Edwards, Goglia, Rice and Smith, "A Study of the Atomization of Liquids", National Defense Research Committee, Div. 10, OSRD No. 6345, Oct. 10, 1945.

18. Haenlein, "Disintegration of a Liquid Jet", NACA T.M. 659, 1932.

19. Bishko, H. & Freudenthal, B. R., "Atomization of Fuel Oil", M.S. Thesis, M.I.T., Course X, 1925.

20. Leising & Rice, "Flame Propogation in Fuel Oil Sprays", M.S. Thesis, M.I.T., Course XIII-A, 1946.

21. Pfieffer, Murati & Engel, "Mixing of Gas Streams", M.S. Thesis, M.I.T., Course XIII-A, 1945.

22. Esso Laboratories Progress Report on "Study of Combustors for Supersonic Ram-Jet", Period April 1, 1946 - June 30, 1946. (CONFIDENTIAL).

Thesis 6501
E6 Erkenbrach
Air atomization of
fuel oil.